ERDC/GSL TR-03-15

US Army Corps of Engineers®
Engineer Research and Development Center

Environmental Security Technology Certification Program

Applications of Synthetic Aperture Radar (SAR) to Unexploded Ordnance (UXO) Delineation

Janet E. Simms

August 2003

Geotechnical and Structures Laboratory

Environmental Security Technology Certification Program

ERDC/GSL TR-03-15
August 2003

Applications of Synthetic Aperture Radar (SAR) to Unexploded Ordnance (UXO) Delineation

Janet E. Simms

Geotechnical and Structures Laboratory
U.S. Army Engineer Research and Development Center
3909 Halls Ferry Road
Vicksburg, MS 39180-6199

Final report

Prepared for U.S. Army Corps of Engineers
Washington, DC 20314-1000

Monitored by Environmental Security Technology Certification Program
901 North Stuart Street, Suite 303
Arlington, VA 22203

ABSTRACT: The Environmental Security Technology Certification Program (ESTCP) provided funding to determine the feasibility of using a foliage penetration (FOPEN) synthetic aperture radar (SAR) system to delineate unexploded ordnance (UXO) contaminated areas. The FOPEN SAR system was developed under a program funded by the Defense Advanced Research Projects Agency(DARPA), Army, and Air Force. The U.S. Army Engineer Research and Development Center coordinated the project efforts, which included participation of the Massachusetts Institute of Technology Lincoln Laboratory, Duke University, and the U.S. Army Research Laboratory. The objective was to measure UXO target signatures in varying target placement conditions, including target orientation, proximity to other targets, and foliage coverage. Three target sizes were imaged; 155-mm projectiles and simulants representing a 2000-lb bomb and 500-lb bomb. Large targets (bomb-size) and dense collections of smaller (155-mm) targets can be detected by the UHF FOPEN SAR when located on the ground surface within sparsely vegetated areas. Multiple aircraft headings will likely increase the chance of imaging UXO. Trees proximal to targets degraded the target resolution and no targets under foliage were able to be resolved. Environmental restrictions at the test site (Camp Navajo, Arizona) prohibited the burying of targets so no statements regarding the FOPEN SAR imaging capabilities of buried UXO can be made. The FOPEN SAR is not optimized for UXO detection. Optimizing the frequency range of a SAR system and exploiting polarization and angle-dependent scattering features may allow separation of UXO from clutter.

Table of Contents

List of Figures

List of Tables

Acronyms

ARL	Army Research Laboratory
ATD	Advanced Technology Demonstration
BDU	Battle Dummy Unit
CECOM RDEC I2WD	Communications-Electronics Command Research, Development & Engineering Center Intelligence & Information Warfare Directorate
DARPA	Defense Advanced Research Projects Agency
ERDC	Engineer Research and Development Center
ESTCP	Environmental Security Technology Certification Program
FOPEN	Foliage Penetration
HH	Co-polarized; both transmitted and received signal are horizontally polarized
HV	Cross-polarized; transmitted signal horizontally polarized, received signal vertically polarized
ITAR	International Traffic in Arms Regulations
MIT/LL	Massachusetts Institute of Technology Lincoln Laboratory
MLFMA	Multi-level Fast Multipole Algorithm
PWF	Polarimetric Whitening Filter
QC/QA	Quality Control/Quality Assurance
RCS	Radar Cross Section
SAR	Synthetic Aperture Radar
SERDP	Strategic Environmental Research and Development Program
T/C	Peak target to mean clutter ratio
UHF	Ultra High Frequency
UXO	Unexploded Ordnance
VHF	Very High Frequency
VV	Co-polarized; both transmitted and received signal vertically polarized

Acknowledgements

The U.S. Army Engineer Research and Development Center (ERDC) was requested to coordinate the efforts of a project funded by the Environmental Security Technology Certification Program (ESTCP). The coordination was undertaken by the Geotecnical and Structures Laboratory (GSL), ERDC, Vicksburg, MS. The project involved evaluating a foliage penetration (FOPEN) synthetic aperture radar (SAR) system to determine its feasibility of measuring unexploded ordnance (UXO) signatures and delineating UXO contaminated areas. This report represents the coordinated efforts of the Massachusetts Institute of Technology Lincoln Laboratory (MIT/LL), Army Research Laboratory (ARL), and Duke University. The FOPEN SAR system was being developed and tested under a program sponsored by the Defense Advanced Research Projects Agency (DARPA), Army, and Air Force. Mr. Lee Moyer was the FOPEN SAR Program Manager for DARPA, and Dr. Jeffery Marqusee was Director, ESTCP.

This report was prepared by Dr. Janet E. Simms, Geosciences and Structures Division (GSD), GSL. The work was performed under the direct supervision of Dr. Lillian D. Wakeley, Chief, Engineering Geology and Geophysics Branch, GSD, and the general supervision of Drs. Robert L. Hall, Chief, GSD, and David W. Pittman, Acting Director, GSL.

At the time of publication of this report, Commander and Executive Director of ERDC was COL James R. Rowan, EN, and Director was Dr. James R. Houston.

Abstract

The clearing of areas contaminated with unexploded ordnance (UXO) is the Army's highest priority Environmental Restoration problem. The Department of Defense (DoD) currently spends millions of dollars annually on UXO cleanup efforts. Initial evaluation of a UXO contaminated area involves the review of historical documents, surface walkovers of randomly chosen areas, and statistical modeling to estimate the ordnance in place. Presently, there are no efficient and cost-effective means of estimating the extent of contamination at UXO sites. The foliage penetration synthetic aperture radar (FOPEN SAR) involved in an Advanced Technology Demonstration (ATD) funded by the Defense Advanced Research Projects Agency (DARPA) has the potential for delineating ordnance impact areas at a fraction of the time and cost incurred using current methods and technology.

The FOPEN SAR is an ultra wide band system that utilizes lower frequencies to achieve foliage penetration. The system has a VHF frequency range of approximately 20 to 70 MHz and UHF range of about 200 to 500 MHz. Its basic operating principle involves transmitting pulsed radio frequency waves and receiving the echoes scattered from targets and the ground surface. The echoes are subjected to analog preprocessing, digitized, and further digitally processed to produce the final imagery. It is a fully polarimetric (HH, VV, HV) side-looking radar.

A test grid containing three target sizes was established to determine the feasibility of using the FOPEN SAR to delineate UXO ranges. The targets were 155-mm projectiles and items representing 500- and 2000-lb bombs. Each type of target was arranged in grids of sparse, moderate, and dense arrays in an open field with low ground cover. Some targets were placed under trees. No targets were buried because of environmental restrictions on Camp Navajo, Arizona.

The primary objective of the demonstration was to measure UXO target signatures in various settings with a secondary objective of determining if the FOPEN SAR has applications for UXO range delineation. The FOPEN system is capable of imaging the larger targets in the sparse array in the open field. The 155-mm projectiles are clearly observable as a cluster in the imagery in dense arrays in the open field. None of the targets located under trees appear to be visible in the images. The bandwidth of the FOPEN SAR does not appear to be suitable for delineating UXO ranges.

Since this work was an add-on to a DARPA sponsored project, there was no direct involvement with regulatory issues.

Applications of Synthetic Aperture Radar (SAR) to Unexploded Ordnance (UXO) Delineation

Geotechnical and Structures Laboratory
U.S. Army Engineer Research and Development Center

June 2003

1. Introduction

1.1 Background Information

1.1.1 Project Motivation. The development of a foliage penetration (FOPEN) synthetic aperture radar (SAR) system is currently being funded under a joint advanced technology demonstration (ATD) program involving the Defense Advanced Research Projects Agency (DARPA), Army, and Air Force. The FOPEN ATD program solicited other agencies to participate in preliminary test flights of the FOPEN SAR system that may have applications for the FOPEN SAR technology. The Environmental Security Technology Certification Program (ESTCP) funded this project to determine the feasibility of using a FOPEN SAR system to delineate unexploded ordnance (UXO) contaminated areas.

1.1.2 Project Participants. The U.S. Army Engineer Research and Development Center (ERDC) Geotechnical and Structures Laboratory (GSL) was responsible for coordinating the efforts of the Massachusetts Institute of Technology Lincoln Laboratory (MIT/LL), Army Research Laboratory (ARL), and Duke University. A point of contact for each organization is provided in Appendix A. MIT/LL performed QC/QA on the data provided by Lockheed Martin, developers of the FOPEN SAR system, and also processed the data to generate imagery used in the modeling efforts. The algorithms used to simulate synthetic aperture radar scattering from individual UXO were developed by Duke. These algorithms were employed by ARL to generate synthetic aperture radar imagery to model the signatures of UXO.

The information in this report is extracted from the final reports provided by the project participants. No imagery is included in this report because of the International Traffic in Arms Regulations (ITAR) classification of the data. The final reports of each participant will be submitted to ESTCP under separate cover [1, 2, 3]. Those reports that contain imagery ([1] and [3]) are not approved for release without permission from DARPA.

1.1.3 Project Overview. The clearing of areas contaminated with UXO is the Army's highest priority Environmental Restoration problem. The Department of Defense (DoD) currently spends millions of dollars annually on UXO cleanup efforts. Initial evaluation of a UXO contaminated area involves the review of historical documents, surface walkovers of randomly chosen areas, and statistical modeling to estimate the ordnance in place. Presently, there are no efficient and cost-effective means of estimating the extent of contamination at UXO sites. The foliage penetration synthetic aperture radar (FOPEN SAR) has the potential for delineating ordnance impact areas at a fraction of the time and cost incurred using current methods and technology.

The resolution of a radar antenna is dependent on the antenna length; the larger the antenna the better the resolution. A SAR is mounted on an airborne or spaceborne platform and takes advantage of the motion of the antenna to achieve an apparent antenna length, or aperture, greater than its actual length. As the antenna moves along a flight path, successive echoes are received from the same target that may be processed to give spatial resolution as if the antenna were as long as the distance the antenna moved when receiving the target echoes. Thus the terminology "synthetic aperture radar" is used to describe the radar system.

Atmospheric conditions such as clouds and rain do not significantly degrade the SAR signal. However, the presence of foliage (trees, brush, grasses) can greatly attenuate the transmitted signal, resulting in a decrease or loss of target resolution. The foliage penetration FOPEN SAR utilizes lower frequencies to "see" through the foliage. Presently, DARPA is funding development and testing of a FOPEN SAR system for the purpose of imaging vehicles beneath tree cover.

Ordnance firing ranges are located in a variety of topographic conditions, including areas of flat and hilly land with tree cover, tall brush, high grasses, or a low vegetated cover. The majority of UXO and ordnance waste within a range are generally distributed in clusters as a result of the controlled firing exercises. This material can range in depth from the surface to a few meters, depending on the ordnance type. The ability to detect a target using SAR is dependent on the material type, size, depth of burial, and angle at which the target is illuminated by the radar. Numerous surface and/or shallow buried ordnance clustered within an area should provide a "target" visible to the FOPEN SAR, thus allowing delineation of impact areas. Widely scattered ordnance located on the fringes of a range may not be detectable by SAR, especially if the items are small. It is possible that the FOPEN SAR may also be applicable for detecting burial pits used to dispose of UXO and ordnance waste. These pits would be buried at shallow depths and have a large concentration of metal that would provide an excellent target for the SAR.

An airborne system that is capable of delineating UXO impact areas under different topographic environments and provide reliable results is highly desirable. Such a system has the potential of saving the DoD millions of dollars when considering the number of UXO contaminated sites in existence. The FOPEN SAR system, or a modified version of it, is a viable candidate for reducing costs and increasing efficiency in the delineation of UXO impact areas.

1.2 Official DoD Requirement Statement(s)

This project addresses the Tri-Service Environmental Quality Research, Development, Test, and Evaluation Strategic Plan, UXO requirements, and more specifically, the U.S. Army Requirement A(1.6a), titled: Unexploded Ordnance (UXO) Screening, Detection, and Discrimination [4] and described the FY99 Army Environmental Requirements and Technology Assessments (AERTA). This Army requirement has been ranked as the highest priority user need in the Environmental Cleanup Pillar. In addition, this project addresses the UXO detection and discrimination requirements and recommendations described in the Defense Science Board Task Force Final Report on UXO Clearance and Remediation published in 1998 [11] and will provide data to support the development of more accurate estimates of the overall DoD UXO environmental remediation costs.

1.2.1 How Requirement(s) Were Addressed. This project addresses the detection of large-scale UXO contaminated areas to support development of more rapid data acquisition systems for estimating the level of contamination. Such a system would ultimately reduce UXO remediation costs.

1.3 Objectives of the Demonstration

The objective of this study is to determine the feasibility of using an airborne SAR system for the delineation of UXO impact areas. Successful deployment of a foliage penetration SAR would allow statistical analysis of the data to determine ordnance density. Based on the analysis, areas within the impact range could be prioritized for remediation purposes.

1.4 Regulatory Issues

There are regulatory issues regarding the transmitted frequency bandwidth of the airborne SAR system and flight paths. However, since this project was not involved with acquisition of the data, it did not have to address these issues.

1.5 Previous Testing of the Technology

No prior test data are available. This report describes data collected during the first scheduled preliminary test of the FOPEN SAR.

2. Technology Description

2.1 Description

The FOPEN SAR is an ultra-wide band system that utilizes lower frequencies to achieve foliage penetration. Its basic operating principle involves transmitting pulsed radio frequency waves and receiving the echoes scattered from targets and the ground surface. The echoes are subjected to analog preprocessing, digitized, and further digitally processed to produce the final imagery.

The system is operated in one of two modes—spot or strip. In spot mode, the radar is focused on a single point and data are gathered at different angles as the aircraft flies over the area. An image 3 km by 3 km is typically obtained in spot mode. Strip mode differs from spot mode in that the radar viewing angle is held fixed and a swath of ground is imaged along the flight path. Strip mode produces a 2-km by 7-km image. Image resolution varies but is typically less than 1 m for both modes. The data acquired during this test were collected in strip mode.

The FOPEN SAR is a fully polarimetric (HH, VV, HV) side-looking radar. Although the exact operating parameters cannot be given, a general range is given in the following tabulation.

	Frequency Range	Integration Angle	Resolution
VHF	20 – 70 MHz	40 to 50 deg	< 10 m
UHF	200 – 500 MHz	30 to 40 deg	< 1 m

2.2 Strengths, Advantages, and Weaknesses

The primary advantage of using an airborne-based system is the ability to acquire a large amount of data covering a wide area in a relatively short period of time. Current methods for estimating the extent of a UXO contaminated site are multi-phase efforts, ground-based, and generally require several weeks/months to complete a site evaluation. With an airborne SAR, the timeframe could be reduced to days. Although the FOPEN SAR system can rapidly gather data over a large area, it was designed to detect large tactical vehicles and its resolution limits the size of UXO that can be detected. Ordnance are typically found in clusters within the primary radius of a firing range so a cluster of smaller UXO, that individually is not detectable, may be imaged. However, on the fringes of a range where the distribution of UXO is sparse, only the larger ordnance may be detected.

2.3 Factors Influencing Cost and Performance

This project was not involved in the design and operation of the FOPEN SAR system so there were no hardware cost concerns. However, Lockheed Martin (LM) supplied the data and their preliminary data processing routines produced phase artifacts in the data. Although the real-time processing LM utilized may not be a concern when detecting vehicle-size targets, it can have a much greater impact when trying to resolve smaller, ordnance-type targets. MIT/LL reprocessed the data using an algorithm that required more time, however, the improvement in image focus justified the increase in time and cost.

3. Site/Facility Description

3.1 Background

This work is an add-on to the primary project funded by DARPA involving the development of a foliage penetration SAR system, therefore, it was not involved with selection of the demonstration site located at Camp Navajo, Arizona. Concerns for the FOPEN SAR include unrestricted flight paths, minimum radio frequency (RF) interference, roads covered by a foliage canopy, roads accessible to large vehicles, and a large area consisting of both open field and tree cover for calibration purposes. In addition to site accessibility, site characteristics desirable for a SAR system specifically designed for UXO detection are low-loss soil for maximum signal penetration; areas having long, short, and no vegetation; tree covered areas; burial of items allowed; and a UXO firing range on the installation or availability of inert UXO at or near the installation.

The Calibration and Open Field aim point used to calibrate the FOPEN SAR system was chosen to construct the UXO test grids. Prior to establishing the UXO test grids in July 2001, a site visit to Camp Navajo occurred in May 2001 to determine suitability of the Calibration and Open Field aim point for the UXO test grids and to identify an area within the aim point for the UXO grids. Also accomplished during that visit was the selection of ordnance items and quantity required for the test. The tabulation below gives the number of each ordnance used.

Selections for UXO Test Grids

Ordnance Item	Quantity
2000-lb Bomb (BDU)	13
500-lb Bomb (half BDU)	11
155-mm Projectile	108

The soil at this site is described as a silty clay loam, and laboratory dielectric measurements indicate it to be a low-loss soil. At the time of testing, the ground was covered with a short grass and there were tree-covered areas bordering the open field test area. This vegetated state allowed data collection under the best- and worst-case foliage scenarios. Camp Navajo is a National Guard facility where some UXO are stored. The ordnance items available at the installation were suitable for this project. Unfortunately, because of environmental restrictions, digging was not allowed at the site so imaging of buried UXO could not be evaluated.

3.2 Site/Facility Characteristics

Camp Navajo is located within Coconino County in the town of Bellemont, AZ, approximately 13 km (8 miles) northwest of Flagstaff. The Calibration and Open Field aim point is located in the northwest region of Camp Navajo (Figure 1). Within the aim point, an area approximately 400 m by 100 m was selected for the UXO test site (Figure 2). Figure 3 provides a panoramic view of the area within the aim point chosen for the test site. Large open spaces were available to establish the test grid with isolated tress within the grid and clusters of trees along the southern border available for foliage cover.

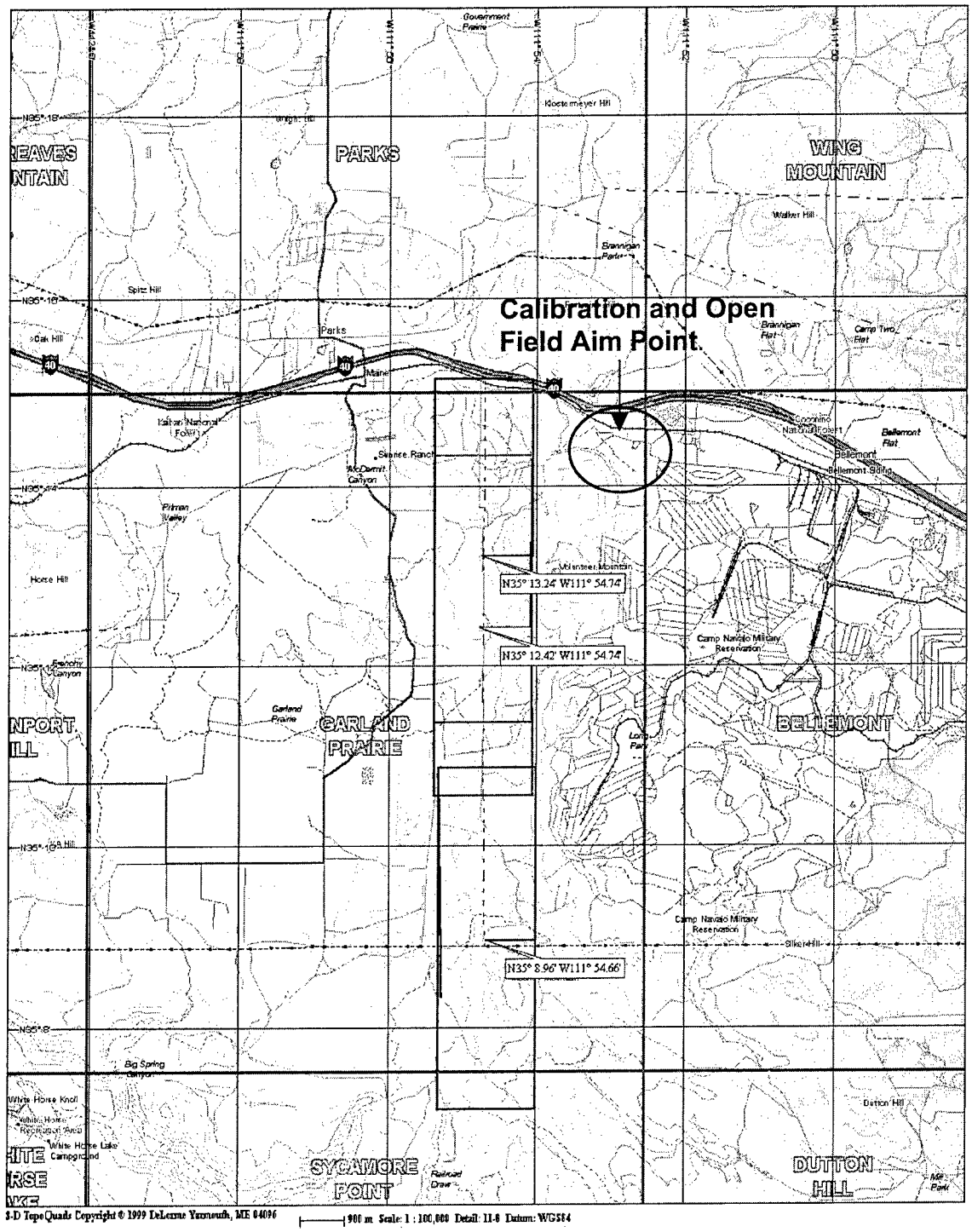

Figure 1. Location of Calibration and Open Field aim point on Camp Navajo, Arizona

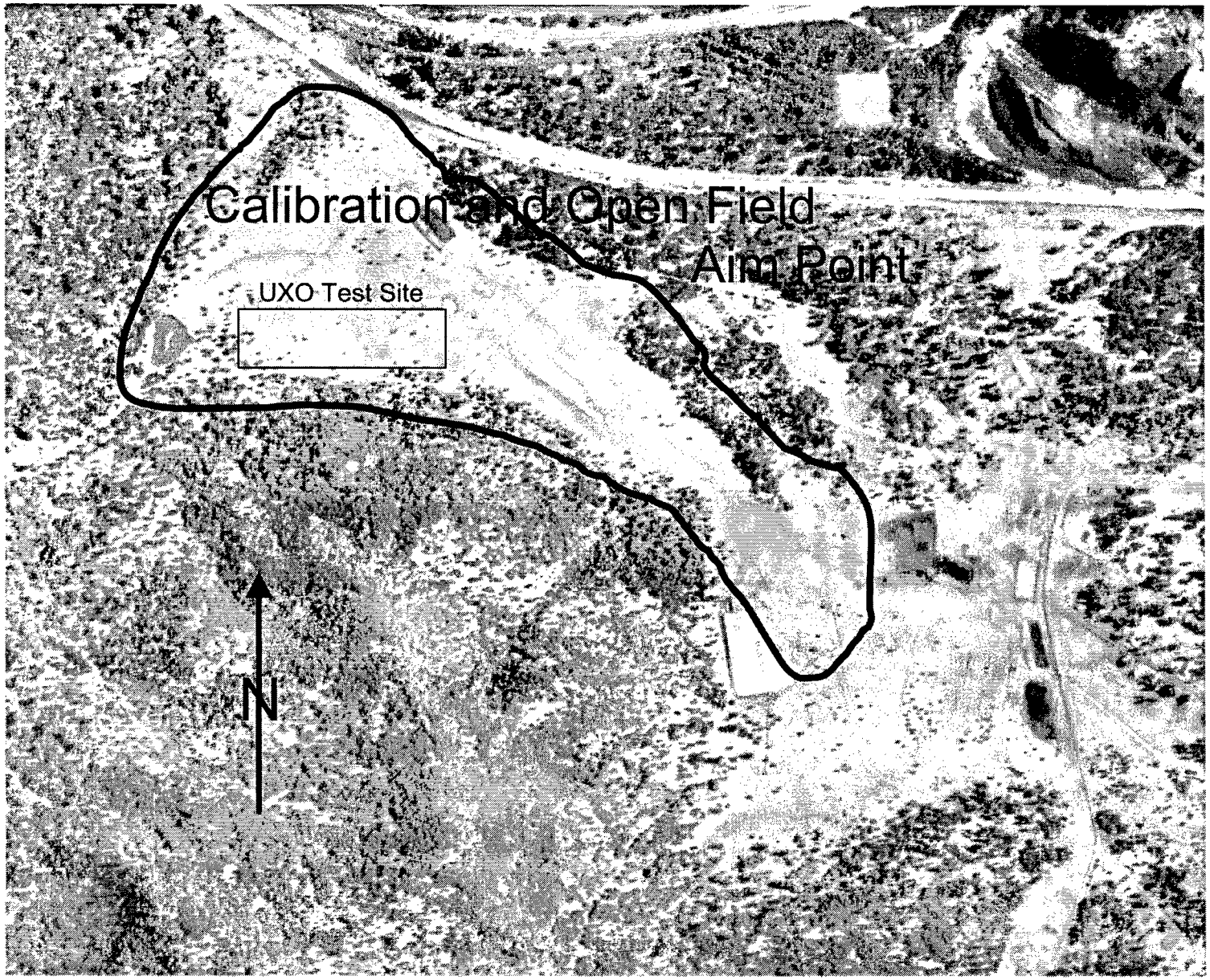

Figure 2. General location of the UXO test grid within the Calibration and Open Field aim point

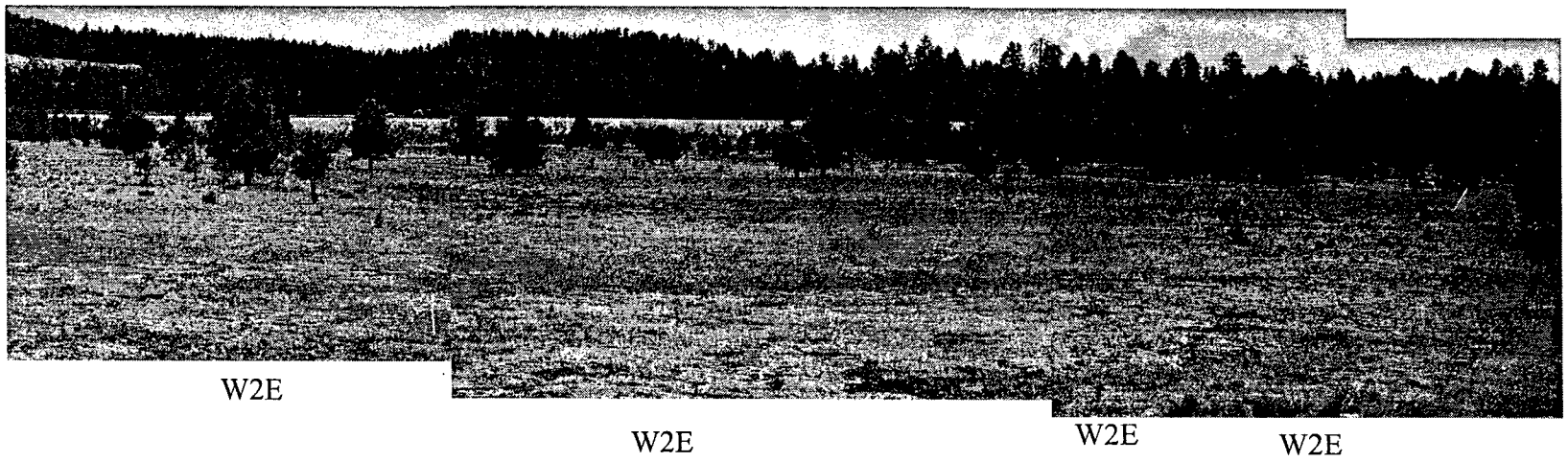

Figure 3. Panoramic view of UXO test site. View is west to east

4. Demonstration Approach

4.1 Performance Objectives

The performance objective was to measure UXO target signatures in varying target placement conditions. The placement conditions include target orientation, proximity to other targets, and foliage coverage. Three sizes of UXO were measured: 2000-lb bomb, 500-lb bomb, and 155-mm projectile. A battle dummy unit (BDU) was used to simulate the 2000-lb bomb (Figure 4), whereas the 500-lb bomb was represented by the front section of a BDU (Figure 5). The targets were placed on the ground surface in grids ranging from a high density of UXO to only one item. These target and clutter data were compared to electromagnetic model data generated using the same UXO placement and Camp Navajo soil parameters.

4.2 Physical Setup and Operation

The UXO test plot encompassed an area approximately 300-m by 75-m. Five grid areas were established. Three of the grid areas contained different arrangements of the 155-mm projectile, 500-lb bomb, and 2000-lb bomb. One area was a random arrangement of UXO and miscellaneous metal, whereas the other was an arrangement of the three ordnance types placed under trees (Figures 6 and 7). The 155-mm grid consisted of five 5-m by 5-m subsections with the density of ordnance ranging from 1 to 54 projectiles per subsection (Figure 8). The 500-lb bomb grid contained three 5-m by 5-m subsections (Figure 9), whereas three 10-m by 10-m subsections were used for the 2000-lb bombs (Figure 10). The randomly arranged grid was 10 m by 10-m and contained three 155-mm projectiles, several lengths of rebar, aluminum vent pipe, metal plates, and razor-wire (Figure 11). Figure 12 shows the placement of UXO under trees.

All grid subsections were oriented north-south and sufficiently spaced to avoid image interference between sections. Camp Navajo personnel assisted with transportation of the ordnance to the test grid and placement of the ordnance in the grids. A flatbed truck was required to haul to the site the large number of items emplaced, and a forklift was used to initially place the ordnance in the grid subsections. Once the ordnance were on the ground they were manually shifted to their final position. Setup of the test grids was accomplished in 2 days.

4.3 Sampling Procedures

Three sizes of UXO were chosen to aid in determining the feasibility of utilizing an airborne SAR system for delineating UXO contaminated areas. Relatively high confidence was placed in the ability to image the larger UXO (2000-lb and 500-lb bombs), but it was questionable if the 155-mm projectile could be seen, especially if isolated. Each type of ordnance was arranged in subsections with the density of items ranging from high, where there was less than an ordnance-length between items, to having just a single ordnance in a subsection (Figures 8 through 12).

The following tabulation gives the number of subsections and items within each subsection for each ordnance type. Within a subsection containing multiple items, the ordnance were arranged at azimuths of 0, 30, 45, 60, or 90 deg. The number of items oriented at 0 deg in each grid was

Number of Items Within Each Grid Subsection						
		Subsection				
Grid	No. of Subsections	1	2	3	4	5
2000-lb Bomb	3	7	5	1	----	----
500-lb Bomb	3	6	4	1	----	----
155-mm Projectile	5	54	32	13	5	1
Random	1	17	----	----	----	----

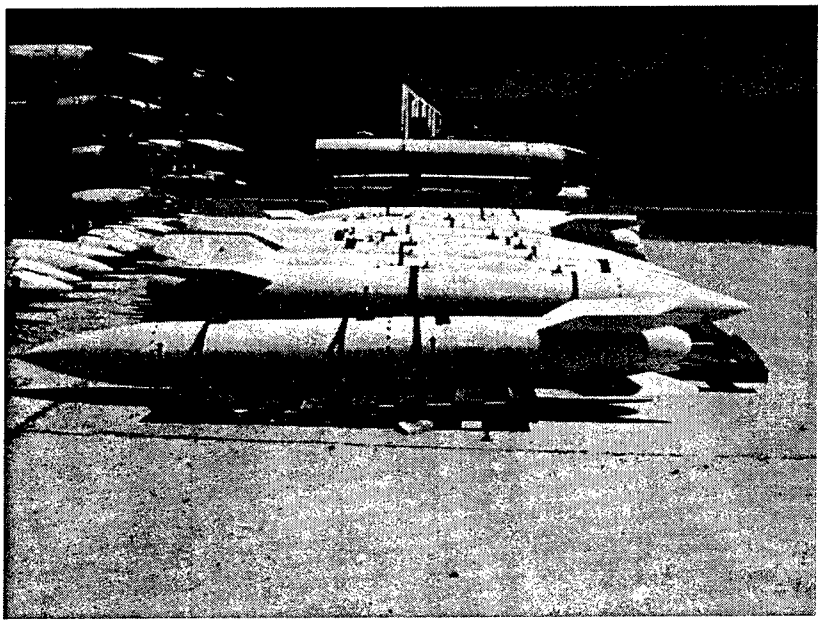

Figure 4. BDU used to simulate 2000-lb bomb

Figure 5. Nose section of BDU used to simulate 500-lb bomb

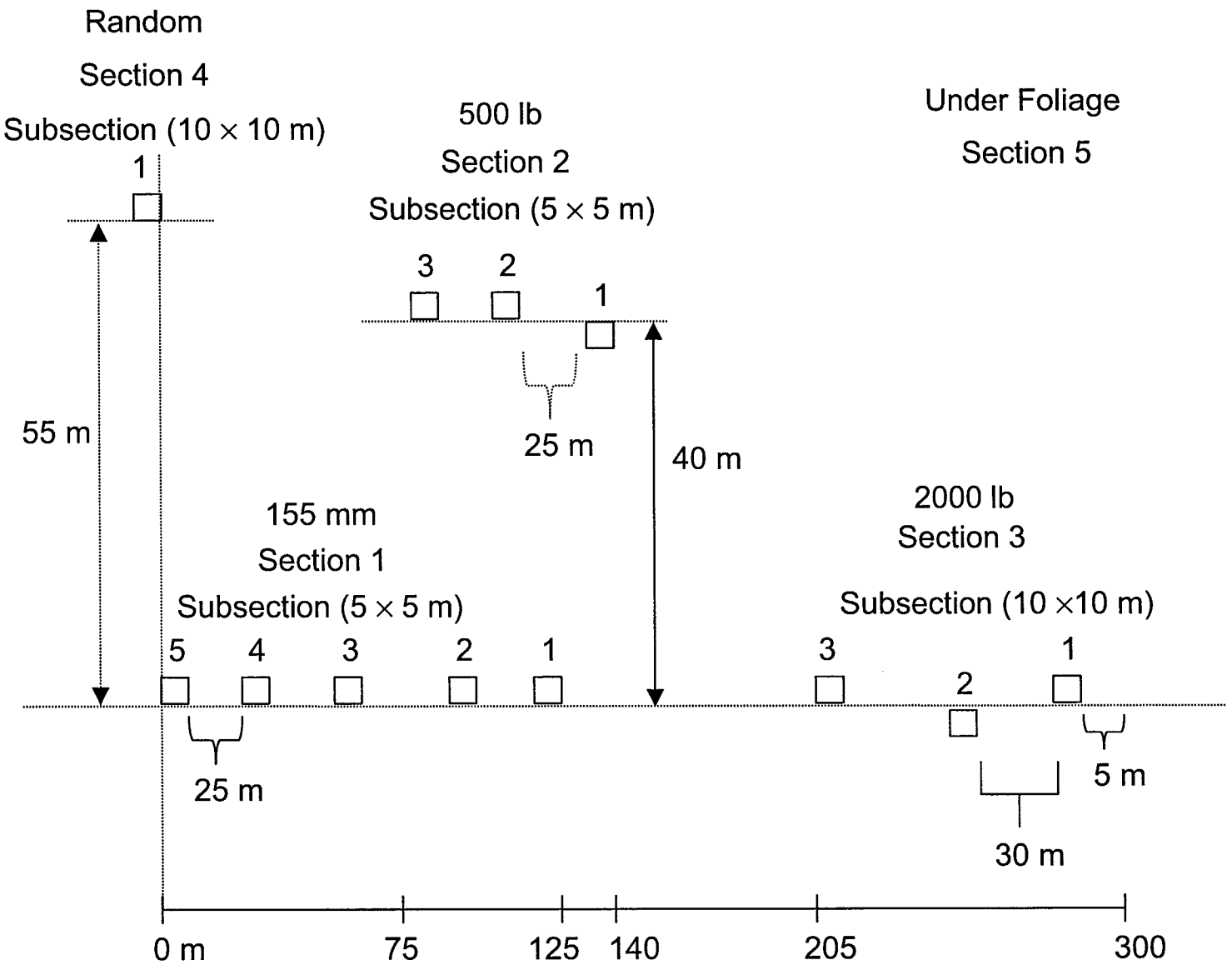

Figure 6. Schematic of UXO test grid

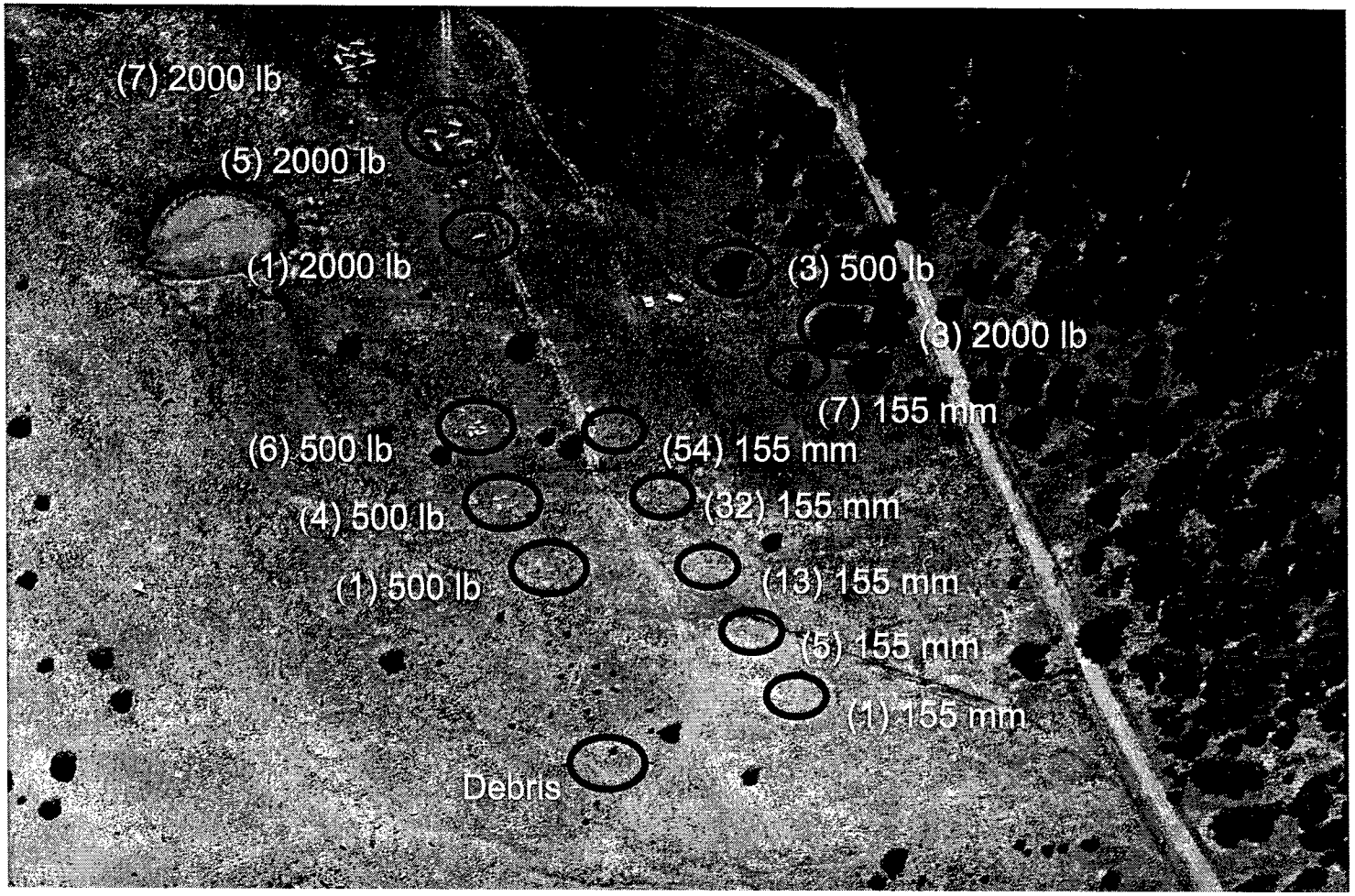

Figure 7. Aerial photograph of UXO test grid and placement of UXO. Numbers in parentheses indicate the number of ordnance in a subsection

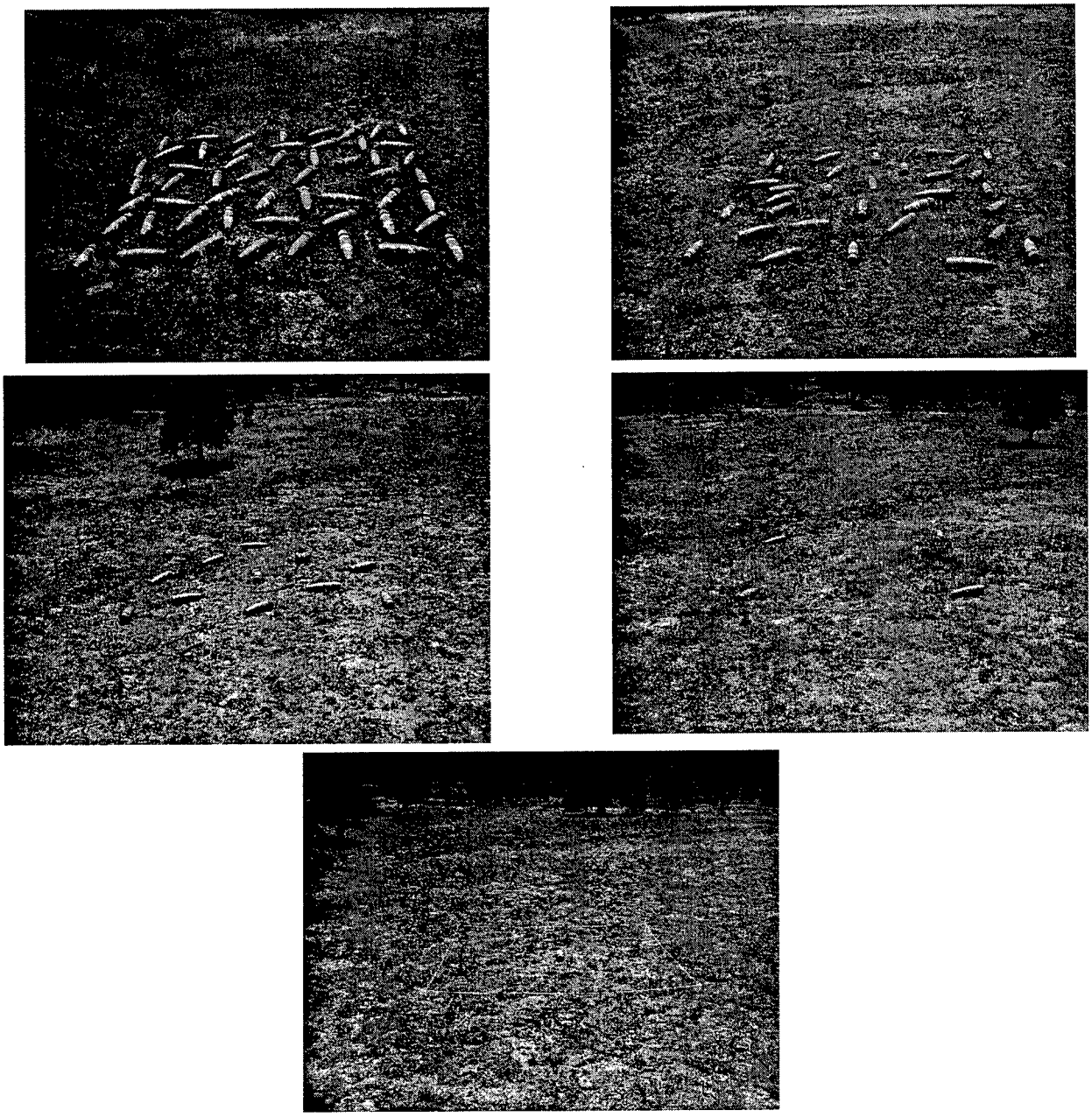

Figure 8. Five subsections of 155-mm projectiles. Subsection 1 contains 54 projectiles; subsection 2 contains 32 projectiles; subsection 3 contains 13 projectiles; subsection 4 contains 5 projectiles; and subsection 5 contains 1 projectile

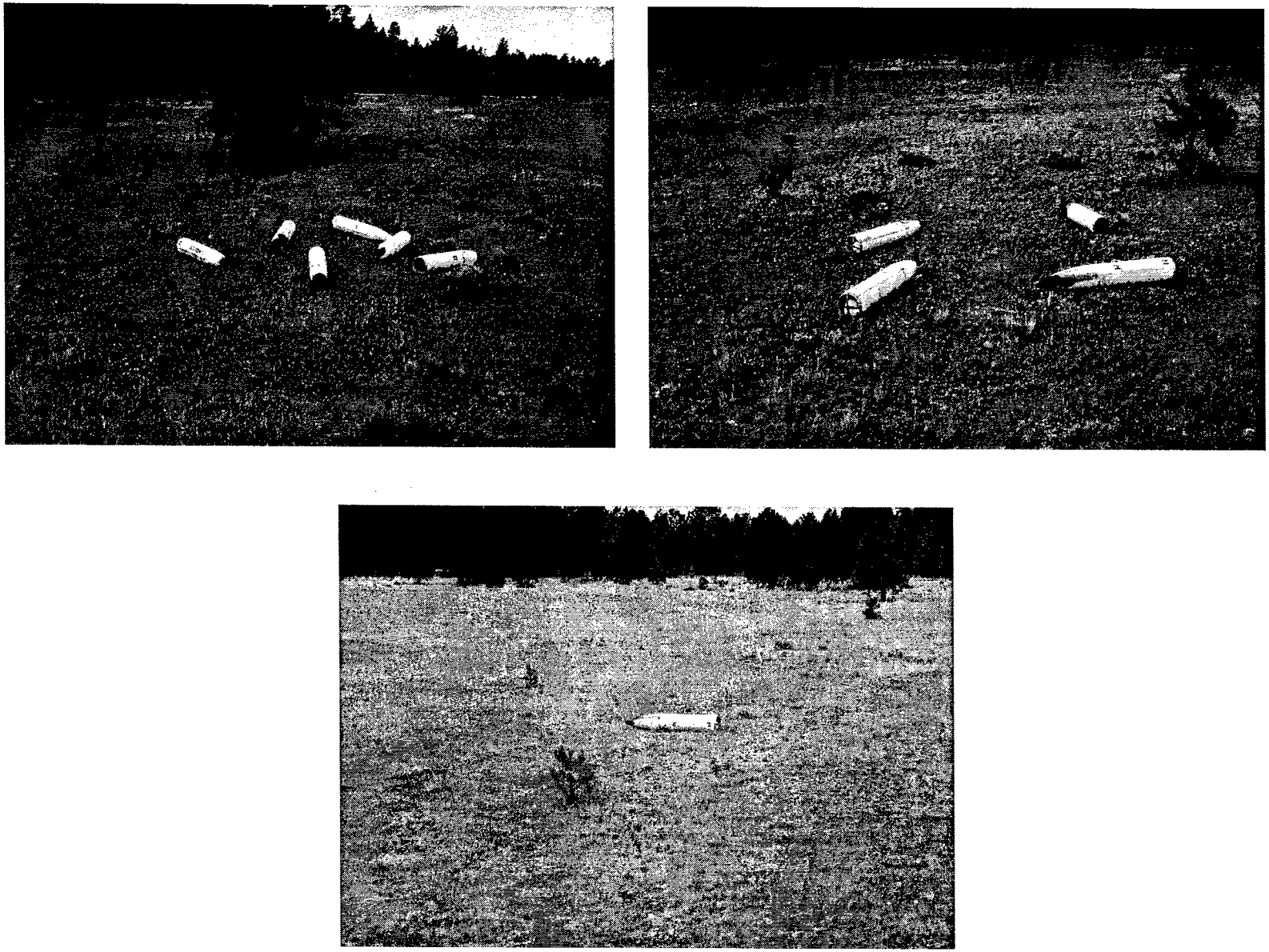

Figure 9. Three subsections of 500-lb bombs (half BDUs). Subsection 1 contains six items; subsection 2 contains four items; and subsection 3 contains one item

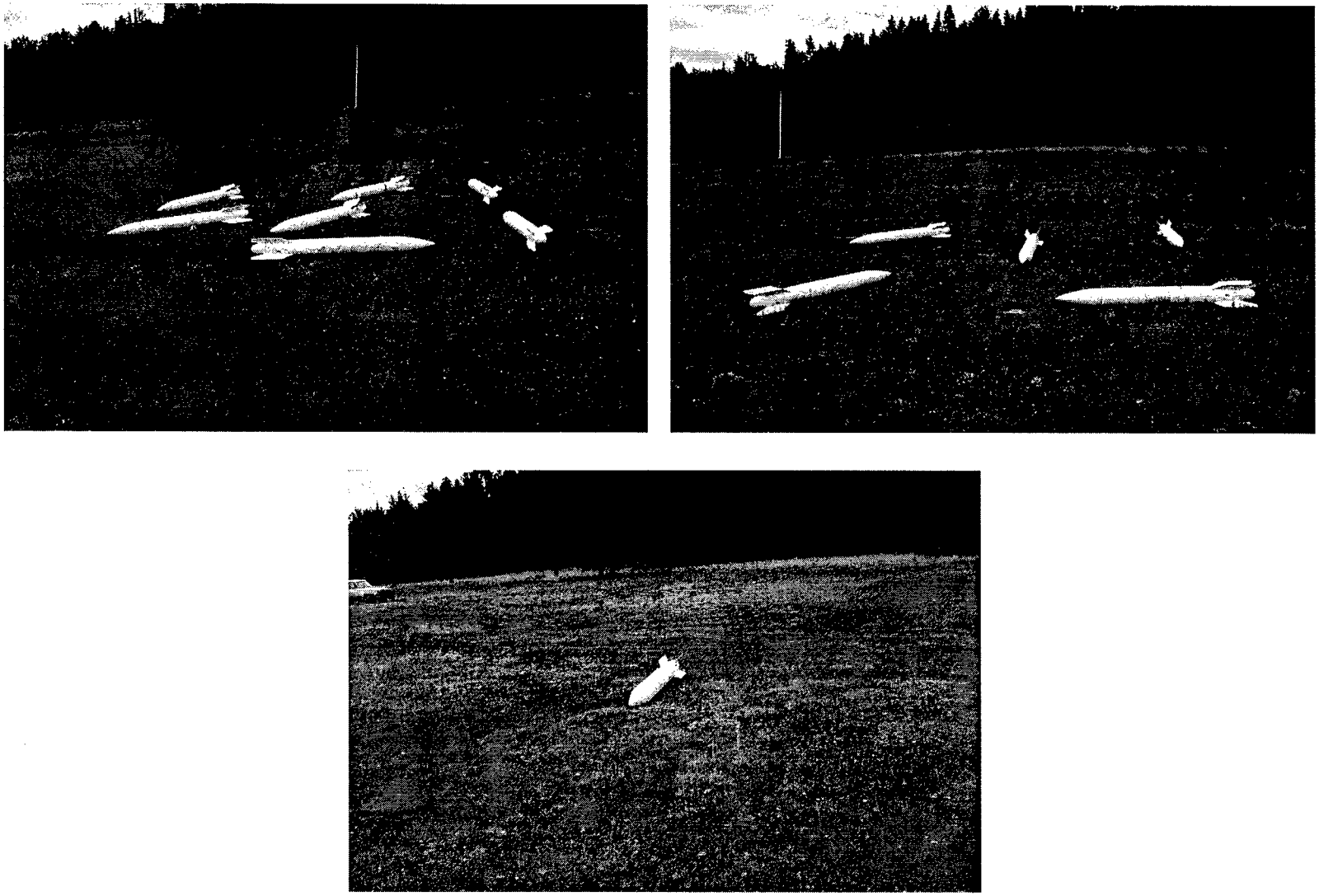

Figure 10. Three subsections of 2000-lb bombs (BDUs). Subsection 1 contains seven items; subsection 2 contains five items; and subsection 3 contains one item

Figure 11. Random (or Debris) grid containing 17 items, three of which are 155-mm projectiles

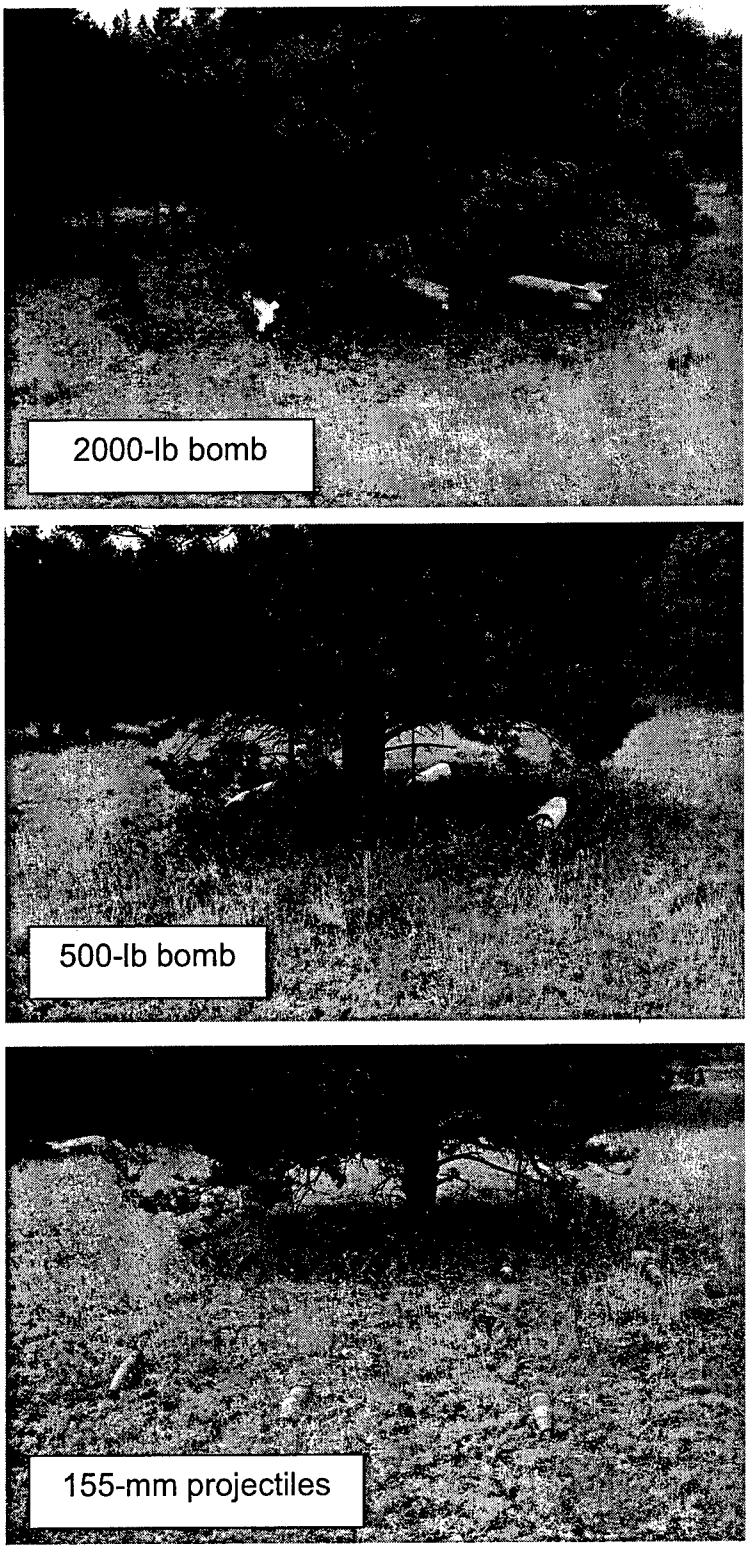

Figure 12. Placement under foliage of 2000-lb bomb (3 items), 500-lb bomb (3 items), and 155-mm projectiles (8 items)

about twice that at the other azimuths. The purpose of different azimuths is to determine if a target is detectable when its long axis orientation is not aligned with the direction of maximum SAR signal radiation. The maximum radar illumination occurs when the radar is broadside to the target, i.e., the flight path parallels the long axis of the target. Besides varying the target azimuth, data were also collected at different flight directions. A total of five passes were flown over the UXO test area at flight headings of 0, 30, 45, and 270 deg with a duplicate pass flown at 0 deg. (Note: a 0-deg flight heading corresponds to a radar heading oriented broadside to a north-south oriented target). A depression angle of 30 deg was used, the maximum angle available for the Calibration and Open Field aim point. The various flight directions aid in determining the ability of the SAR system to detect UXO at low (270-deg), moderate (45-deg), and high (0-deg) radar cross section (RCS) levels (relative to a north-south oriented target).

The first flight of the Option 2 collection by Lockheed Martin was labeled OPT2F1 [1]. The UXO test data were collected during flight 16 (F16) of the Camp Navajo collection and labeled OPT2F1 (F16). The naming convention for MIT/LL–processed imagery is a16p#, where 'a' is the ATD sensor, 16 is the flight number, and # is the pass number. Details of the information deliverable by Lockheed Martin are given in the Demonstration Plan [5]. The UXO flight was flown on July 18, 2001. Appendix B provides information regarding archival of the flight data.

MIT/LL was responsible for deploying the calibration array reflectors, collecting soil samples, surveying the UXO deployment, procuring lookdown aerial photographs of the collection area, collecting ground photos of each ordnance deployment array, and collecting ground station global positioning system (GPS) data.

Calibration targets were utilized as control points for the UXO flight data. A total of 23 targets were deployed. The types of targets include triangular trihedrals, triangular dihedrals, and square trihedrals. The quantity and size of each is summarized in the following tabulation.

Calibration Targets Deployed					
	Quantity				
Calibration Target	43 in. (1.1 m)	4 ft (1.2 m)	8 ft (2.4 m)	16 ft (4.9 m)	
Triangular trihedral	2	2	11	3	
Triangular dihedral	----	----	----	----	3*
Square trihedral	----	----	3	----	

* 1 each: 45-, 67.5-, 90-deg roll

Ground truth data collection involved the collection of ground and aerial photographs of UXO deployment sites. The photographs include an aerial photograph of the collection site and ground photographs of the 2000-lb bomb deployments, 500-lb bomb deployments, 155-mm projectile deployments and the debris (or random) deployment. Aerial photographs were collected by Southwest Aerial Photo. The approximate resolution of the aerial photographs is 1:6400.

Survey data were collected for each UXO. Coordinates in WGS84 latitude and longitude and NAVD88 elevation were recorded. The coordinates for the UXO 2000-lb bomb, 500-lb bomb, 155-mm projectile, and debris deployments are listed in Tables 1 through 4, respectively, of the MIT/LL final report [1]. Also included in each table is the survey point on the UXO and the survey reference number that can be used to reference the image truth data that are distributed with the imagery. Table 5 of the referenced report [1] lists the survey information for the calibration and registration reflectors that were deployed in the area. Also included in Table 5 of reference [1], for each survey point, are the survey reference number, the reflector size and type, and the reflector pointing angle.

Two soil samples were collected by MIT/LL and delivered to Duke, where they were characterized using an open-coax probe and a network analyzer. These measurements were used to yield the frequency-dependent relative complex dielectric permittivity of the soils, $\varepsilon_r = \varepsilon_r' - j\varepsilon_r''$.

4.4 Analytical Procedures

4.4.1 Image Processing [1]. Lockheed Martin was responsible for the data collection and produced SAR images using an omega-k (range migration) technique [6, 7]. With omega-k processing, motion compensation is exact to one point in the image and approximate at other points, causing focus to degrade with large motion error. Results from Lockheed Martin processing are not reported here. MIT/LL images were formed by a fast backprojection technique [8]. Although this method takes longer to process the data than omega-k algorithms, the image focus is better for aircraft flight that is not perfectly straight, as is the case with the FOPEN system. With backprojection processing, perfect focus is possible across the entire image regardless of the aircraft off-track motion error.

Image formation of VHF and UHF SAR data using the fast backprojection algorithm includes radio frequency interference (RFI) rejection, height of focus correction, and calibration. Five data passes were collected over the UXO test area. Preliminary processing was done on all five passes to determine candidate passes for final processing. Preliminary processing used RFI rejection software version 1 (a single binary filter formed from the center of the pass and applied to the entire pass), aircraft position data generated from the autonomous GPS and internal navigation system, and no height of focus correction. As planned, final processing was completed on two passes. Final processing included RFI rejection software version 2 (a bank of binary filters generated across the entire pass and applied to the pulses from which it was generated), aircraft position data generated from differential GPS, height of focus correction, and calibration. A slight improvement in image quality (better focus and reduced residual RFI) is seen in the final images when compared with the preliminary images. The following tabulation lists the processing summary for the UXO flights.

Data Collection Passes for OPT2F1 (F16)			
Pass	AC Heading deg true	Preliminary Processing	Final Processing
1	0	Yes	No
2	30	Yes	Yes
3	45	Yes	No
4	270	Yes	No
5	0	Yes	Yes

4.4.2 Data Modeling [2]. Under previous support from the Strategic Environmental Research and Development Program (SERDP), Duke developed a multi-level fast multipole algorithm (MLFMA) for the analysis of single targets in the vicinity of a half space (soil). One of the important issues in such computational modeling involves mesh generation. In particular, the MLFMA model is based on computing the electric currents induced on the surface of the target (UXO). The surface currents are decomposed in terms of a basis, and the model solves for the basis-function coefficients. The current basis functions are essentially triangular patches used to represent the target surface. Duke developed a mesh-generation package for general UXO shapes and used this model to represent the targets subsequently modeled by ARL. Figure 13 depicts the meshes used to represent the 155-mm projectile, 500-lb bomb, and 2000-lb bomb (BDU-38B-2000). The triangular patch models require a large number of triangles, N, to appropriately model each target, with the tradeoff being accuracy of the modeling versus the amount of memory (related to N^2) and computer time (related to N^3) necessary to evaluate each model. Note that the models used here are reasonable representations of intact UXO but do not include the effects of fins.

One of the important issues to be examined in this study involved the applicability of linearity in the context of SAR scattering from multiple UXO. Duke considered this issue in detail by extending its MLFMA software for modeling an arbitrary number of UXO in the presence of soil. An iterative formulation was developed to model the SAR signature of multiple UXO. Assume for simplicity there are two UXO, UXO1 and UXO2, although the procedure developed is applicable to an arbitrary number of targets. First, compute the currents induced on targets UXO1 and UXO2 in isolation, caused by the fields incident from the sensor (and no interactions *between* the targets). In the next step, the fields incident on UXO1 are represented as the incident fields from the sensor plus the scattered fields from UXO2, where to compute the latter the induced currents on UXO2 from the first step are used. This yields an updated version of the currents induced on UXO1; the currents on UXO2 are updated similarly. This process repeats iteratively until the induced currents converge for both targets. The number of iterations required is dictated by the amount of coupling between the two targets.

ARL took the data from the UXO passes and converted it for use in their in-house ultra wideband (UWB) data quality and focusing programs. The method of moments (MoM) modeling technique was used for this analysis. The MoM models are based on a full-wave formulation of Maxwell's equations and show great promise for detailed three-dimensional (3-D) analysis of reasonably sized targets across a wide frequency range. Electrically large bodies

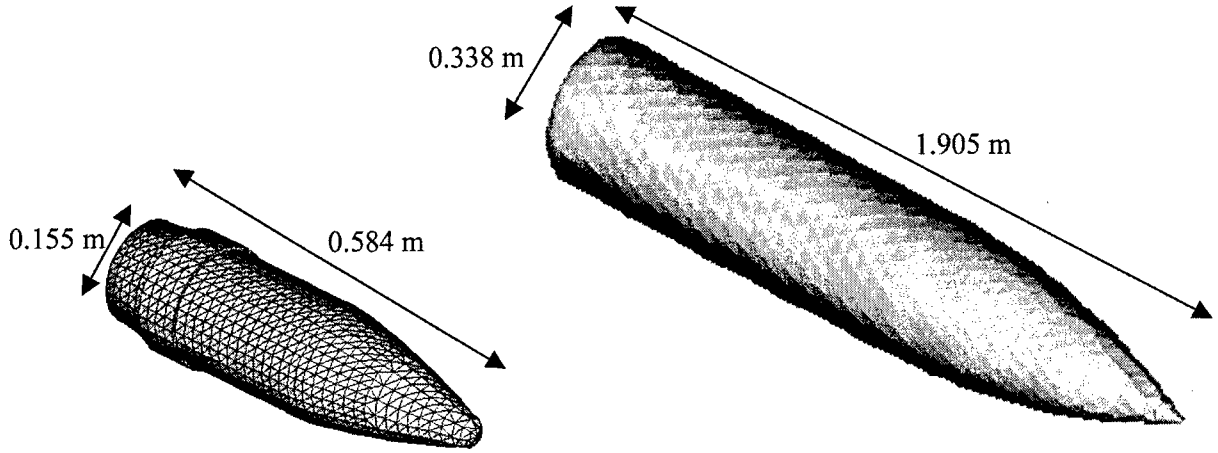

155-mm model (left) and 500-lb bomb model (right)

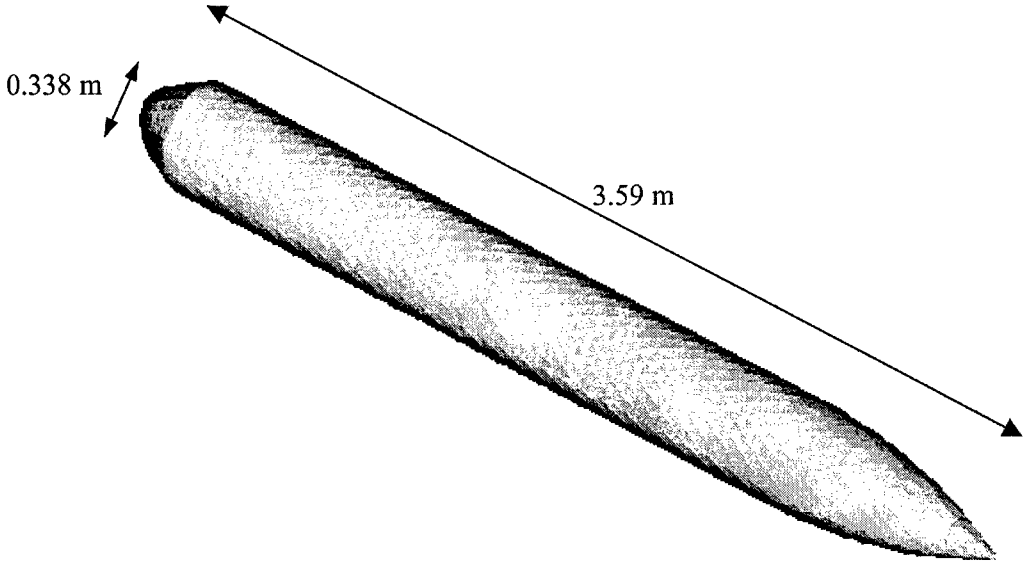

2000-lb bomb model (not to scale)

Figure 13. Triangular patch meshes used to model the UXO

(targets) require many triangular patches to accurately model the surface currents on the body. Once the current has been calculated, the scattered fields and the radar cross section (RCS) can be found directly. MoM codes require regular-sized triangles appropriate for the smallest region to be represented (typically 1/10 of a wavelength). Duke University provided the triangular patch models for the test targets.

5. Performance Assessment

5.1 Performance Data

5.1.1 Imagery—MIT/LL [1]. Imagery of the FOPEN SAR data is not presented in this report because of the ITAR data classification. All imagery provided by MIT/LL will be submitted to ESTCP under separate cover in the MIT/LL final report entitled "FOPEN ATD Camp Navajo UXO Data Collection Summary" [1].

To quantify the image noise levels in the FOPEN ATD imagery, images were formed with the transmitter off data. Results from the UHF noise-only data indicate that the FOPEN imagery is not limited by residual RFI and system noise. The returns measured from the grass regions are consistent with multiplicative noise contamination from tree clutter sidelobes in the grass areas. The range sidelobes are caused by spectral notching of the transmitted signal required to avoid the aircraft instrument landing systems and spectral notching during processing that was required to remove RFI. Results from analysis of the VHF data indicate that backlobe contamination is the main source of residual noise and that the returns from the open grass regions are dominated by the backlobe clutter contamination. Hence, it has been concluded that backscatter measurements from the grass regions indicate the image noise equivalent σ_0 for both UHF and VHF imagery. The UHF average tree backscatter-to-noise ratio (CNR) was 11.0 dB or greater for all polarization channels. The VHF CNR for tree backscatter is approximately 13.0 dB. Tables 1 and 2 summarize the image quality parameters obtained from passes 2 and 5. The pass 2 images contain the calibration array site. Average statistics from the reflectors are also included in Table 1. Appendix C contains a description of a few of the image-related parameters mentioned in the text.

TABLE 1. QC/QA Statistics for FOPEN ATD Data F16 Pass 2 (a16p2) (30 deg)

	UHF			VHF
	HH	VV	HV	HH
Noise equivalent σ_0 (dB)	–20.2	–23.8	–32.4	–32.6
Avg tree backscatter (dB)	–7.5	–12.9	–20.1	–18.7
Range resolution (m)	< 1	< 1	< 8	< 8
Cross-range resolution (m)	< 1	< 1	< 8	< 8
Max range sidelobe level (dB below peak)	–15.8	–14.8	–17.9	–14.9
Max cross range sidelobe level (dB below peak)	–12.7	–16.1	–16.9	–10.2
Calibration uncertainty (dBsm)	2.0	1.1	1.4	1.0
[Reflector peak radar cross section (RCS) variation from theoretical]				

TABLE 2. QC/QA Statistics for FOPEN ATD Data F16 Pass 5 (a16p5) (0 deg)

	UHF			VHF
	HH	VV	HV	HH
Noise equivalent σ_0 (dB)	−19.8	−23.5	−29.7	−31.0
Avg tree backscatter (dB)	−9.2	−13.5	−18.6	−19.1

5.1.1.1 2000-lb Bomb Deployment. Figure 14 shows an example cross-range cut through the peak pixel of the UHF, HH, and VV polarization images of the dense 2000-lb bomb deployment for an aircraft heading of 0 deg. The cut passes through the two visible 2000-lb bombs; the arrows indicate the length of the 2000-lb bomb. The peak dB level measured over the targets is at least 10 dB above the local clutter, suggesting that the targets should be detectable.

A polarimetric whitening filter (PWF) process [9] was applied to the data. To generate the PWF image, the HH, VV, and HV images are whitened, amplitude equalized, and summed. At microwave frequencies this algorithm has been shown to minimize image speckle. PWF reduces the clutter standard deviation and often improves detection performance. The image statistics for the 2000-lb bomb dense deployment with PWF applied are summarized in Table 3. Peak RCS can fluctuate because of calibration variation pass to pass. The T/C (log[peak target to mean local clutter ratio]) removes any pass-to-pass calibration. The T/C was only calculated for the dense target deployments because of time restraints. The larger the clutter standard deviation, the more false alarms obtained. Depending on the distribution of the clutter and the number of

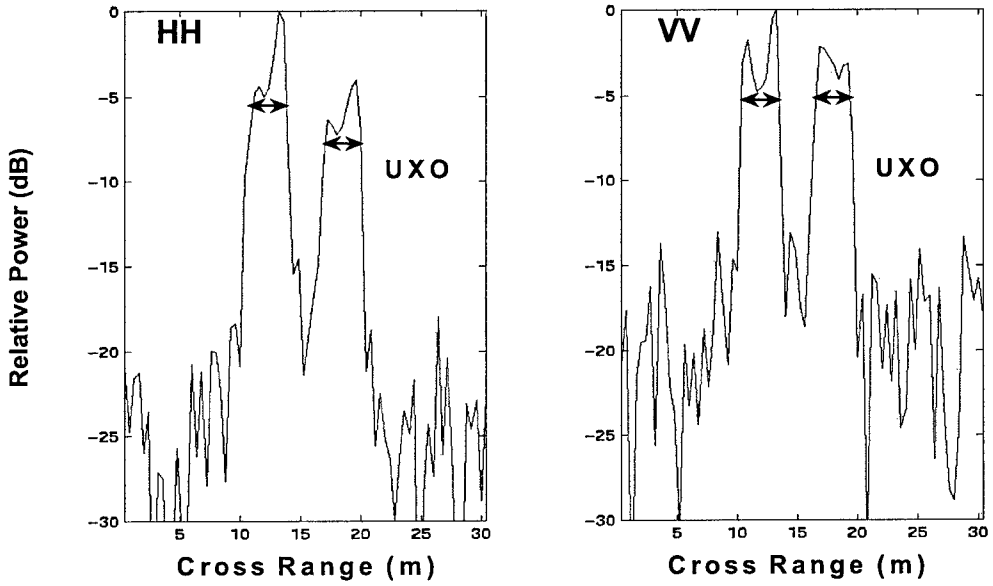

Figure 14. UHF cross-range cut through UXOs from 0-deg aircraft heading image, 2000-lb bomb dense deployment

TABLE 3. 2000-lb Bomb Dense Deployment Peak RCS Statistics for HH, HV, VV, and PWF Data

	Peak RCS dBsm	T/C dB	Clutter Standard Deviation
HH	5.2	26.9	5.9
HV	−12.5	18.3	5.8
VV	0.4	25.0	6.1
PWF	12.0	21.3	3.1

false alarms that could be tolerated, generally the peak target should be $2\sigma_c$ (twice the clutter standard deviation) or more above the mean clutter ($T/C > 2\sigma_c$) for reliable detection. The 2000-lb target dense deployment meets this criterion under these surface conditions. Table 4 lists the peak RCS statistics for all the 2000-lb bomb deployments at both aircraft headings. The peak occurs on different UXOs for each aircraft heading, and generally, the peak occurrs on a target oriented in a direction similar to the aircraft heading. By comparing the RCS values over the different target densities, it is possible to see the variation in RCS with aspect. For example, the sparse deployment contained a single target oriented 0 deg so the peak RCS at that heading is considerably greater than at 30 deg. The dense and medium deployments both had targets oriented at approximately 0 and 30 deg, so similar values of peak RCS are measured. Hence, having *multilook capability would probably improve UXO detection.*

TABLE 4. Peak RCS (dBsm) for 2000-lb Bomb Open Deployments, Aircraft Headings 0 and 30 deg

	HH	VV	HV
Dense (7)			
0°	5.7	1.1	−9.6
30°	5.2	0.4	−12.5
Medium (5)			
0°	6.4	0.3	−9.9
30°	5.2	0.9	−9.4
Sparse (1)			
0°	5.7	−3.3	−11.5
30°	1.9	−8.6	−9.3

For the VHF and HH polarization images of the 2000-lb bomb dense deployment, the peak pixel RCS for the 0-deg aircraft heading is −2.7 dBsm, resulting in a T/C of 12.4 dB. The peak pixel RCS for the 30-deg aircraft heading is −4.7 dBsm, resulting in a T/C of 9.0 dB. The grass backscatter standard deviation is about 5 dB; therefore, *detection of the UXO deployments in this test is expected to be difficult with the VHF data.*

5.1.1.2 500-lb Bomb Deployment. The peak pixel RCS of the 500-lb bomb for the 0-deg aircraft heading is 1.8 dBsm (HH) and −4.4 dBsm (VV), resulting in a T/C of 23.0 dB (HH) and 20.0 dB (VV). The peak pixel RCS of the 500-lb bomb for the 30-deg aircraft heading is −0.1 dBsm (HH) and −5.6 dBsm (VV), resulting in a T/C of 21.6 dB (HH) and 19.4 dB (VV).

Cross-range cuts through the peak pixel of the UHF, HH, and VV polarization images of the 500-lb bomb deployment for an aircraft heading of 0 deg are shown in Figure 15. Arrows indicate the position of the UXO. Since the peak RCS is at least 10 dB above the peak local clutter, the 500-lb targets should be detectable under this scenario. Table 5 summarizes the peak RCS statistics for the various 500-lb bomb deployments. Similar behavior is observed relative to aspect angle as was seen with the 2000-lb targets.

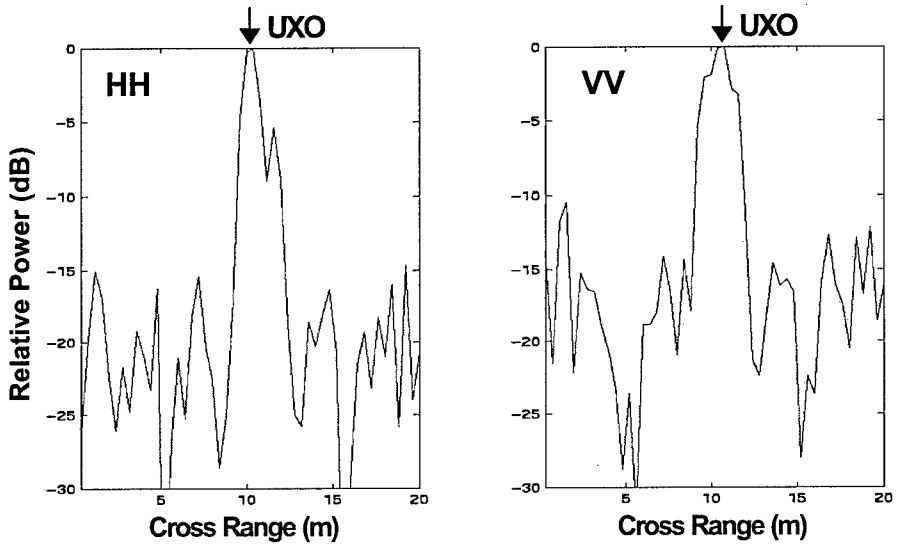

Figure 15. UHF cross-range cut through UXO from 0-deg aircraft heading image, 500-lb bomb deployment

TABLE 5. Peak RCS (dBsm) for 500-lb Bomb Open Deployments

	HH	VV	HV
Dense (6)			
0°	1.8	–4.4	–8.8
30°	–0.1	–5.6	–14.6
Medium (4)			
0°	1.4	–2.0	–14.2
30°	2.5	–6.0	–10.1
Sparse (1)			
0°	0.4	–4.5	–18.0
30°	–5.9	–13.2	–19.2

5.1.1.3 155-mm Projectile Deployment. The peak pixel RCS of the 155-mm projectile for the 0-deg aircraft heading was −3.8 dBsm (HH) and −3.4 dBsm (VV), resulting in a T/C of 18.0 dB (HH) and 20.9 dB (VV). The peak pixel RCS of the 155-mm projectile for the 30-deg aircraft heading was −5.0 dBsm (HH) and −1.2 dBsm (VV) resulting, in a T/C of 17.0 dB (HH) and 23.3 dB (VV). Cross-range cuts through the cluster peak of the UHF, HH, and VV polarization images of the 155-mm projectile deployment for an aircraft heading of 0 deg are shown in Figure 16. The image statistics for the 155-mm projectile deployment are provided in Tables 6 and 7. The T/C is two to four times greater than the clutter standard deviation for each polarization, and six times for PWF, suggesting that the dense arrangement of 155-mm is detectable. However, the clutter background level relative to the target peak is higher (Figure 16) than that for the 2000-lb target (Figure 14) and the 500-lb target (Figure 15), so further analysis is required to determine if the 155-mm dense arrangement would be distinguishable from false alarm sources. Note that in Table 7 the peak RCS values are similar for both aircraft headings for the sparse deployment containing a single target (oriented at 0 deg). This indicates that the background clutter provides a similar level of response as a single 155-mm projectile, so the smaller targets will probably only be detectable in large groupings.

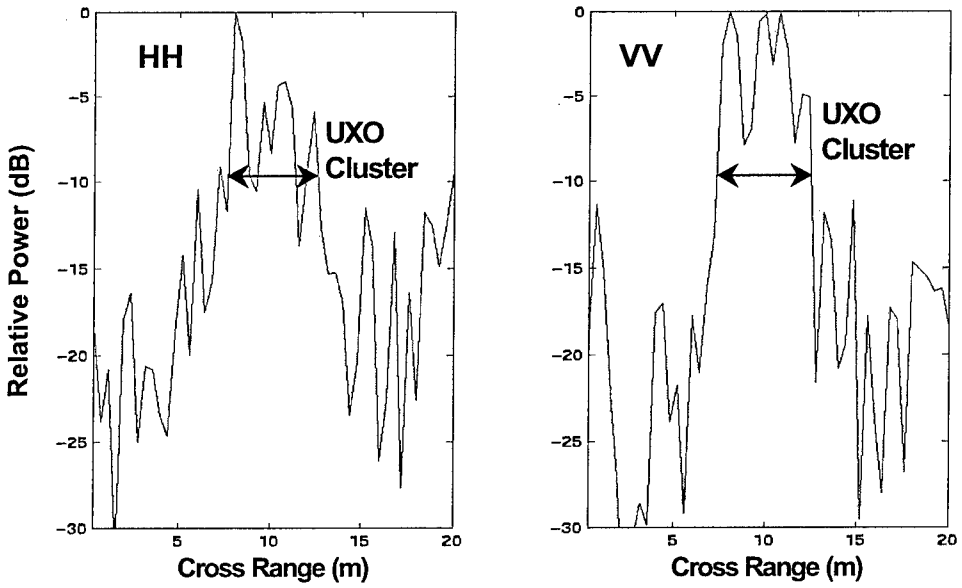

Figure 16. UHF cross-range cut through UXO cluster from 0-deg aircraft heading image, 155-mm projectile deployment

TABLE 6. 155-mm Projectile Peak RCS Statistics for HH, HV, VV, and PWF Data

	Peak RCS dBsm	T/C, dB	Clutter Standard Deviation
HH	–5.0	17.0	5.4
HV	–16.5	13.7	5.7
VV	–1.2	23.3	5.5
PWF	9.0	18.0	3.1

TABLE 7. Peak RCS (dBsm) for 155-mm Projectile Open Deployments Aircraft Headings 0 and 30 deg

Deployment (Number in Cluster)	HH	VV	HV
Dense (54)			
0°	–3.8	–3.4	–14.9
30°	–5.0	–1.2	–16.5
Medium (32)			
0°	–6.9	–5.7	–15.8
30°	–5.6	–5.7	–16.0
Sparse (13)			
0°	–7.2	–6.6	–18.1
30°	–9.7	–9.3	–18.6
Sparse (5)			
0°	–6.9	–7.7	–19.9
30°	–8.4	–9.3	–20.0
Sparse (1)			
0°	–9.9	–10.6	–20.2
30°	–11.7	–13.5	–19.4

5.1.1.4 UXO Deployment Under Trees. Only slight differences in the images are visible between the images acquired prior to placement of the UXO under foliage and after deployment. Those differences are seen in the VV polarization image of the 155-mm projectiles where a few of the projectiles are not under the tree cover. For UXOs in the open but with tree clutter nearby, the T/C could drop by 10 to 12 dB, since the mean tree RCS is about 10 to 12 dB above the mean RCS of the grass. In addition, the RCS of a UXO under trees could drop on average by another 10 dB because of the two-way foliage attenuation at UHF. Hence, based on the available data, *detection of UXO targets that are concealed by trees does not look promising using the FOPEN ATD SAR.*

5.1.2 Soil Analysis. Two soil samples were collected within the UXO test area. They can be described as a silty clay loam. The samples were analyzed to determine their frequency-dependent characteristics as water content was varied. These data were subsequently used in the modeling efforts. The samples are designated Sample 1 and Sample 2. Results are plotted for the following cases: (a) as the soil was in the bag, (b) the soil after it was dried out, and (c) the soil with 5, 10, 15, and 20 percent water, by weight. The results are presented in the set of plots in Figure 17. The soil is considered to be an "average" soil and has moderately lossy dielectric properties.

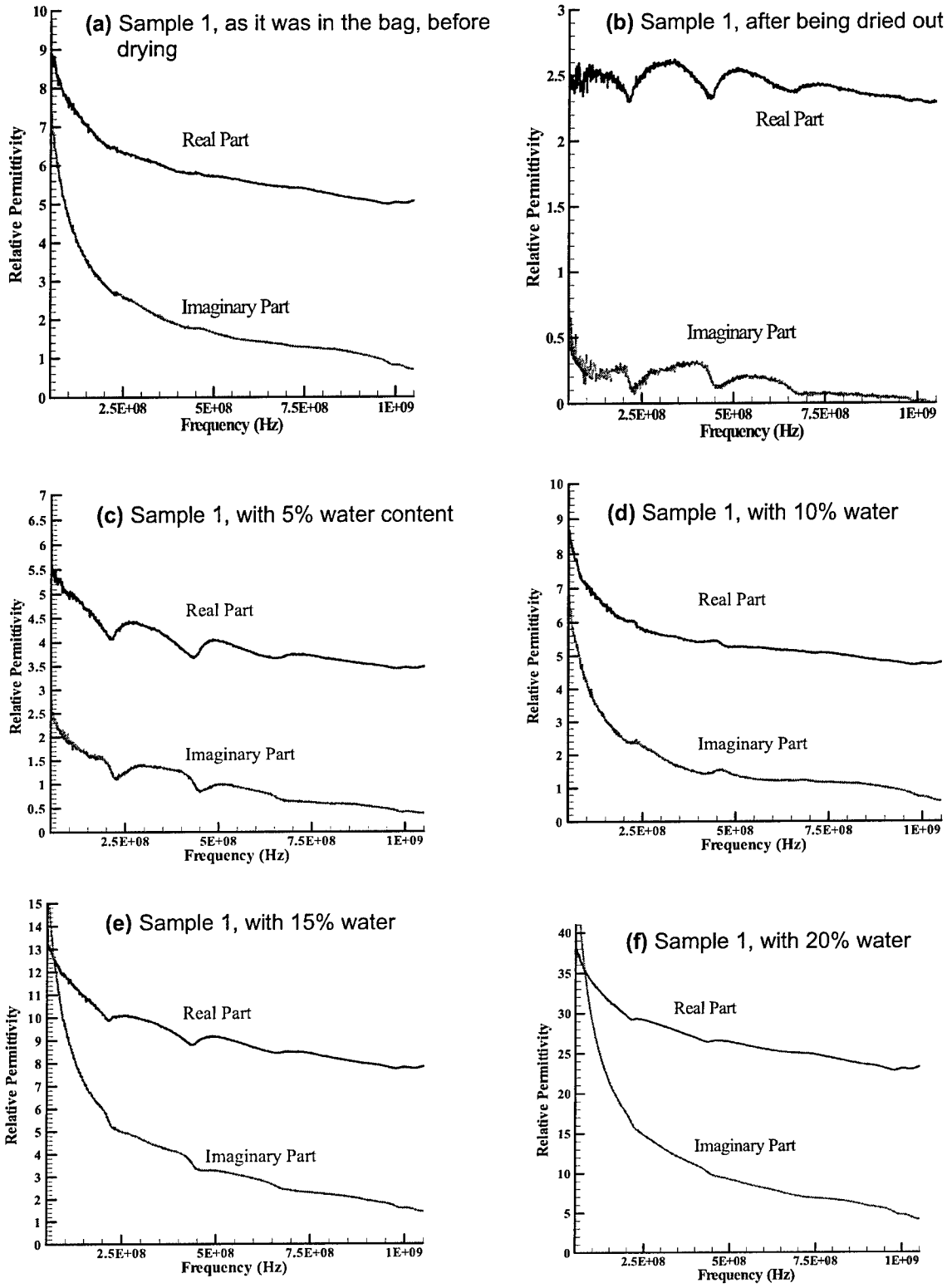

Figure 17. Results of dielectric permittivity measurements on soils collected at Camp Navajo (Continued)

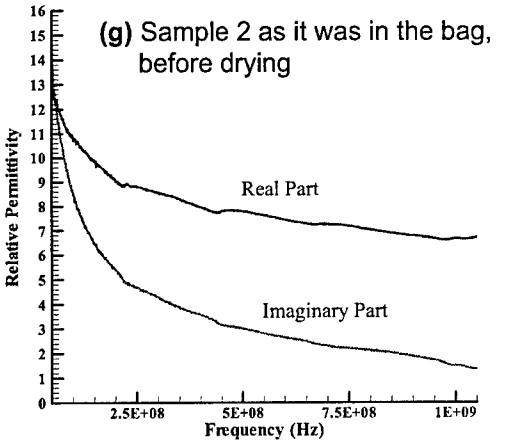

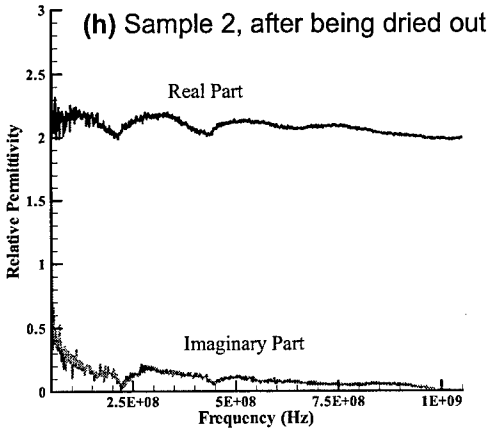

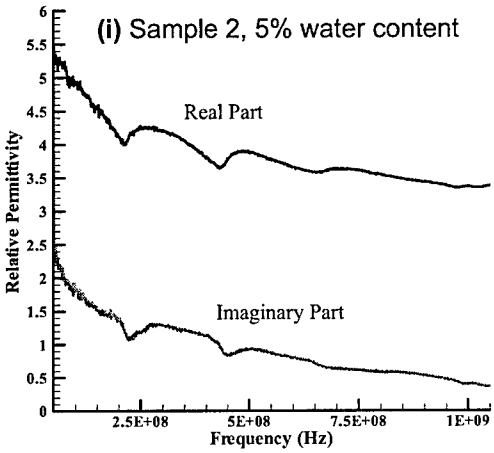

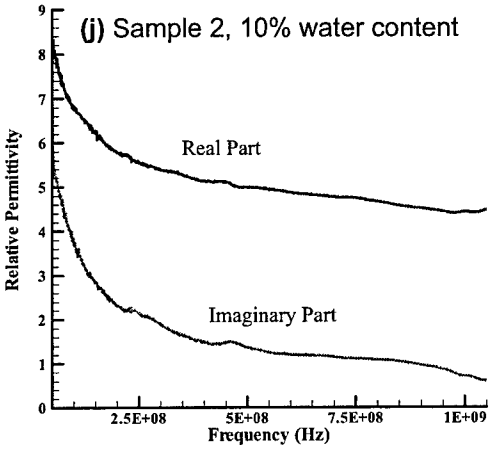

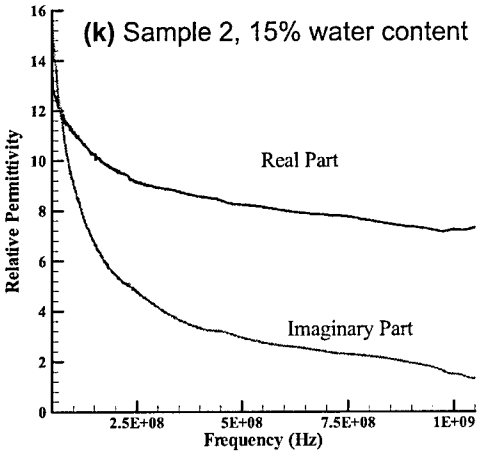

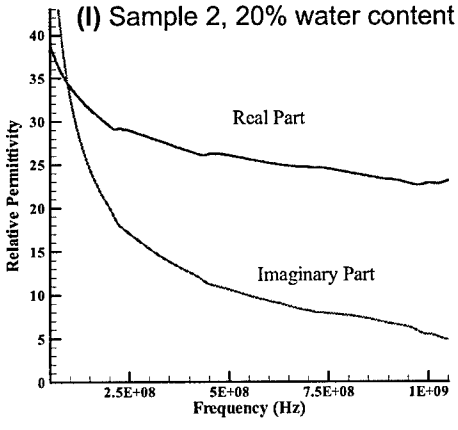

Figure 17. (Concluded)

5.1.3 Data Modeling—Proximal UXO (Duke) [2]. Figure 18 depicts the mesh used to simulate scattering from two UXOs buried in soil, using soil properties characterized by complex dielectric constant $\varepsilon_r = 5 - j0.2$ and conductivity $\sigma = 0.01$ S/m. The incident angles (see coordinate system in Figure 18) are $\theta_i = 60$ deg and $\varphi_i = 120$ deg, and the bistatic scattering angles are $\theta_s = 60$ deg and -180 deg $\leq \varphi_s \leq$ 180 deg. For this example, two sets of results are considered: (a) the RCS computed rigorously, via the iterative formulation discussed above; and (b) the RCS computed by treating each UXO in isolation, and simply adding their signatures (ignoring interaction). The latter approach is expected to yield reasonable results, because the interaction effects are diminished by propagation through the lossy ground. The RCS results in Figure 19, for operation at 600 MHz, indicate that the simple linear-combination (no interactions) model can predict the general RCS variation with angle, although the detailed RCS can be off by several dB. In this example $N_1 = N_2 = 8{,}295$.

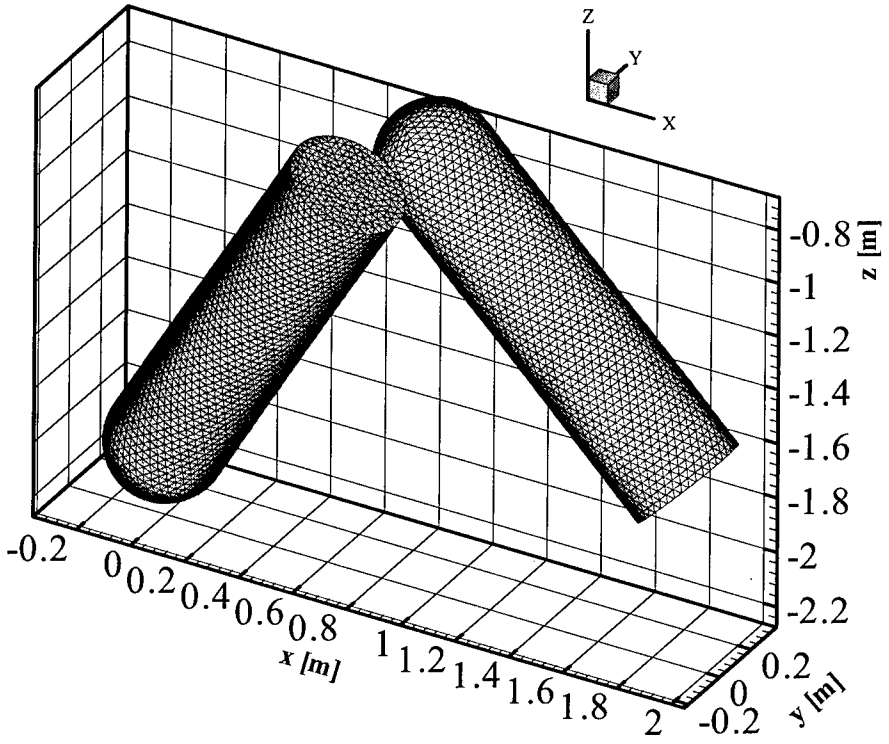

Figure 18. Mesh used to model scattering from two UXOs buried in soil. The soil interface is at $z = 0$

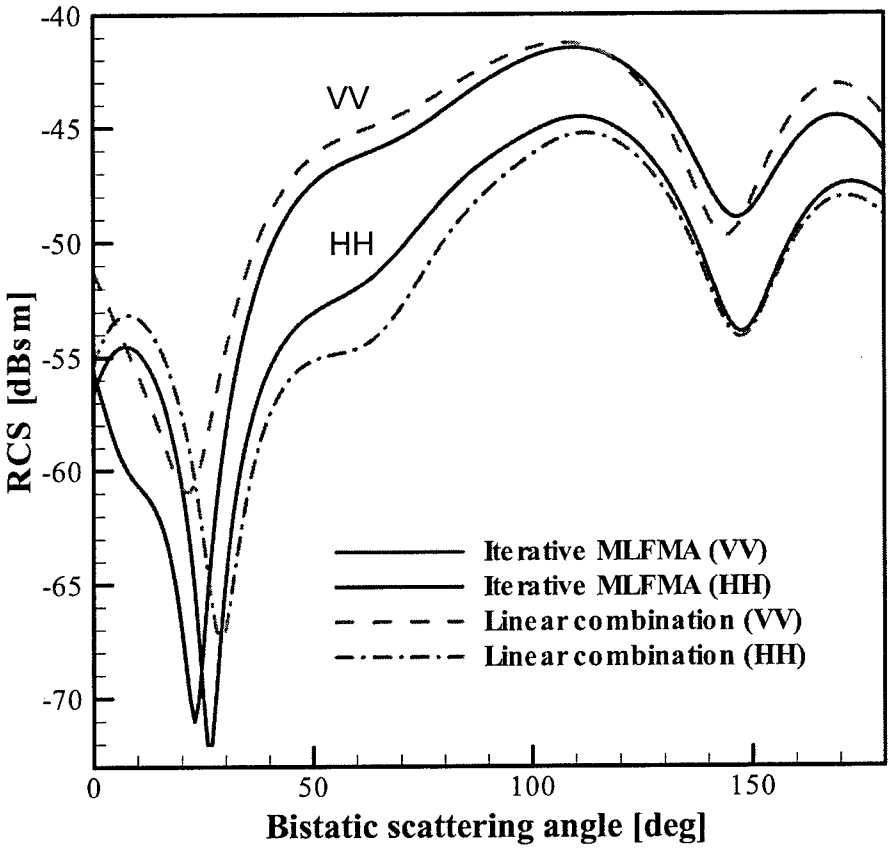

Figure 19. Bistatic RCS for the problem depicted in Figure 18, at 600 MHz. Results are shown when all interactions are accounted for via the algorithm (MLFMA) discussed above, and when the targets are modeled in isolation and simply added

The results in Figure 19 indicate that simple linear addition of the individual target signatures, ignoring inter-target wave interaction, yields excellent agreement with the rigorous solution, in which all interactions are accounted for. Consequently, in the comparisons ARL has done, they have ignored inter-target interactions. The two UXOs in Figures 18 and 19 are relatively closely situated. The model demonstrates the expected reduced coupling as the targets are further separated.

5.1.4 Data Modeling—Electromagnetic Modeling (ARL) [3]. For each target type, subsection three (as described in the Camp Navajo Test Plan [5]) of the target emplacement was used. In the following pages, photos and schematics of the layouts are shown as well as the model predictions for those targets. A flight direction of 270 deg was chosen for these simulations. This places the aircraft south of the target area, westbound with the radar looking to the north. The antenna depression angle used for all the simulations was 30 deg. Each target was analyzed in 1-deg increments across the frequency range of interest using the median values for dielectric constant and conductivity determined for the Camp Navajo site (provided by Duke

University). The calculations were performed on the ARL high performance computers. Because of the sizes of the 500- and 2000-lb targets, the simulations could not be run all the way to 2000 MHz. Thus, in trading off accuracy and computing time, the frequency response of the 500-lb target is limited to 1000 MHz and that of the 2000-lb target is limited to 550 MHz to ensure the data presented are valid.

For each target present in the layout, the equivalent time response for the bandwidth supported by the radar system being modeled is computed. Because of the sensitive nature of the FOPEN data, those frequencies ranges are not explicitly specified here. However, to allow some comparison with the BoomSAR, a general frequency range for the FOPEN VHF is 20 to 70 MHz and FOPEN UHF is 200 to 500 MHz. The BoomSAR bandwidth is 50 to 1200 MHz. These time responses are computed for all those angles within the integration angle space for each of the radar systems being modeled: less than 50 deg for the FOPEN SAR and 60 deg for the ARL BoomSAR (Figure 20). These time responses are then focused into bipolar (signed) imagery for each target. Figure 21 illustrates SAR imagery represented in bipolar and magnitude format. The magnitude image is normally the way most SAR imagery is presented. It is the positive valued envelope of the energy from the bipolar data and is useful for being able to present results in decibels. However, the bipolar data give better insight to the details in the target return and is typically what is used in this data analysis. It is assumed that the targets are sufficiently

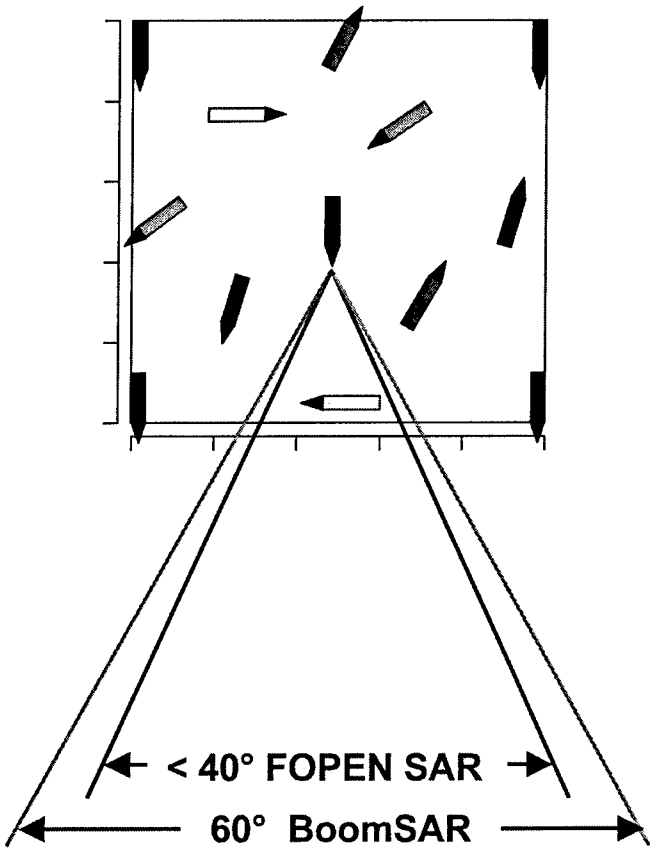

Figure 20. Synthetic aperture integration angle drawn to the center target

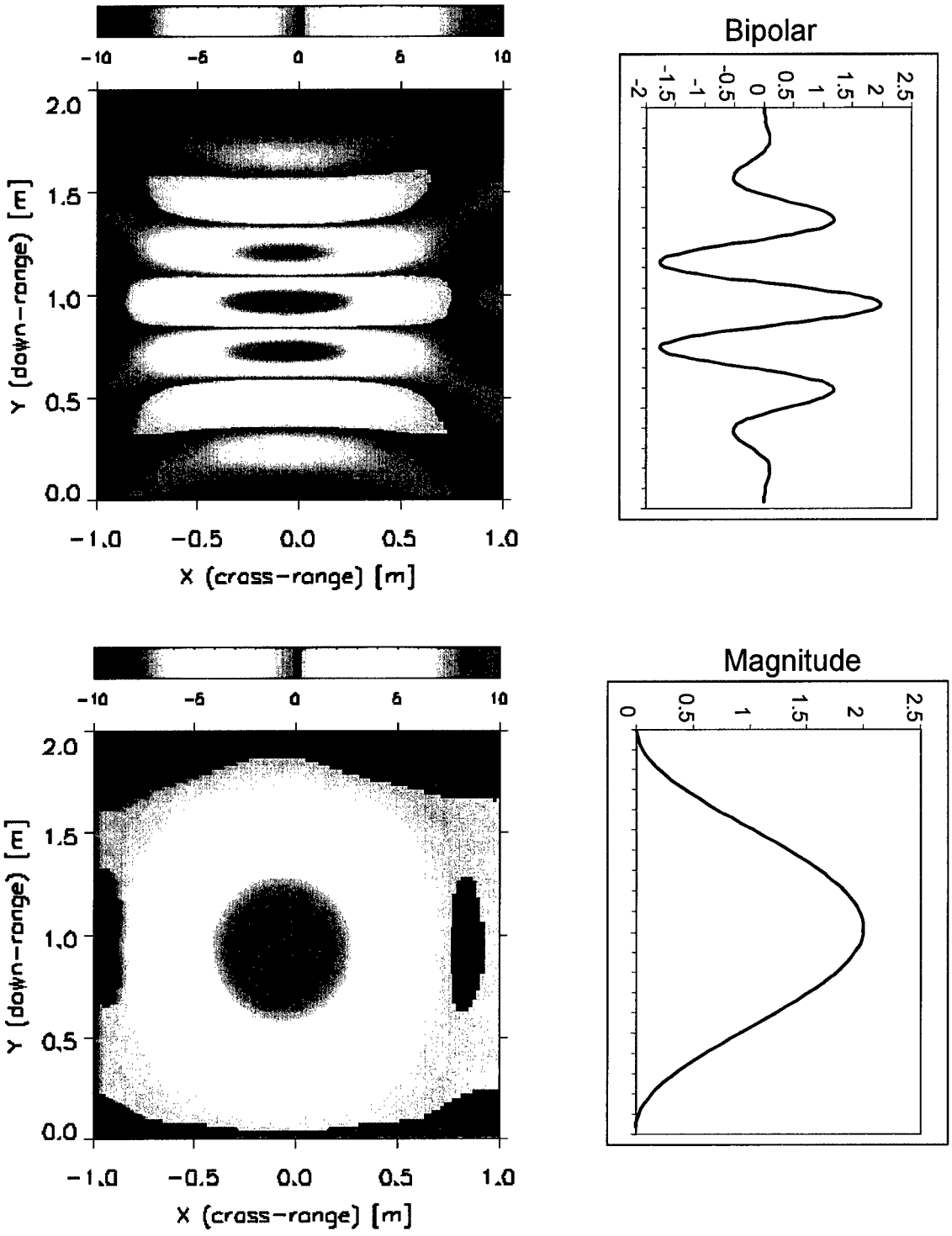

Figure 21. Synthetic data of bipolar and magnitude images for a 155-mm projectile at VHF

separated that the interaction between targets caused by an incident electromagnetic (EM) field is negligible, and another program sums up the responses from all targets, appropriately placed in the layout, to generate the overall image response.

On the following pages are Figures 22 through 34 for the three different target types showing: a photograph of the actual target placement (Figures 22, 27, 31), a graphic target layout (Figures 23, 28, 32), simulated SAR imagery for co-polarized and cross-polarized responses (Figures 24, 25, 29, 33), and the frequency response of the targets at broadside (0-deg), oblique (45-deg), and end on (90-deg) alignments (Figures 26, 30, 34). The frequency coverage for the various radars examined is shown graphically for the last set of these plots. For the 155-mm projectile, an additional set of imagery is provided to compare the response of these targets over Yuma Proving Ground soil to that of the Camp Navajo soil (Figures 24 and 25).

All of these models assume a flat, completely isotropic ground beneath the target with no surface or subsurface irregularities or nearby clutter to perturb the imagery. Also, the model includes no noise or interference the radars may receive (internally or externally generated), since none has been specified. In addition, the models, analytic in nature, exhibit no errors in image formation because of unsensed motion or acceleration that might be present in actual radars. This makes these images very "clean" looking compared to those from actual radars, which might suffer from any or all of the above perturbations to the data. Thus, these results will allow us to understand if the UXO exhibits unique frequency or aspect angle dependent radar scattering behavior that would permit the discrimination of the UXO from clutter objects.

5.1.4.1 Impact of Soil Properties on Surface UXO Signatures. A comparison of Figures 24 and 25 shows there are very few differences between the Camp Navajo soil models and the Yuma soil models. This is not surprising since the targets are above the soil, rather than embedded in it. In addition, recall that the current EM modeling techniques are not accounting for the surface (or volumetric) clutter that may be present. Therefore, although the actual soil electrical properties minimally impact the response from the surface UXO, the level of response from the surface clutter is likely to impact the ability to detect and discriminate surface UXO. This supports the use of the models to build an understanding of the UXO signatures without the surface clutter, so that effective discrimination features can be developed to separate the UXO signature from the surface clutter.

5.1.4.2 Impact of Radar Resolution. There are interesting differences between the BoomSAR models and the FOPEN UHF models. Please note that all of the polarized response plots (Figures 24, 25, 29, 33) are automatically scaled to the largest signal in the image, so a direct comparison of the magnitude of the response in these images cannot be made. A direct comparison would also assume the total power available from both radars is the same. However, this is misleading since the BoomSAR pulse covers a much wider frequency regime.

The frequency bandwidth of the FOPEN UHF waveform is much narrower than the BoomSAR, leading to coarser range resolution. The impact of this can be seen in Figures 24 and 25 where the BoomSAR images are able to resolve the direction of the oblique angled targets. This loss in range resolution in the FOPEN UHF radar leads to an overlapping of target signatures as noted in

Figure 22. Photograph of 155-mm projectile layout at Camp Navajo

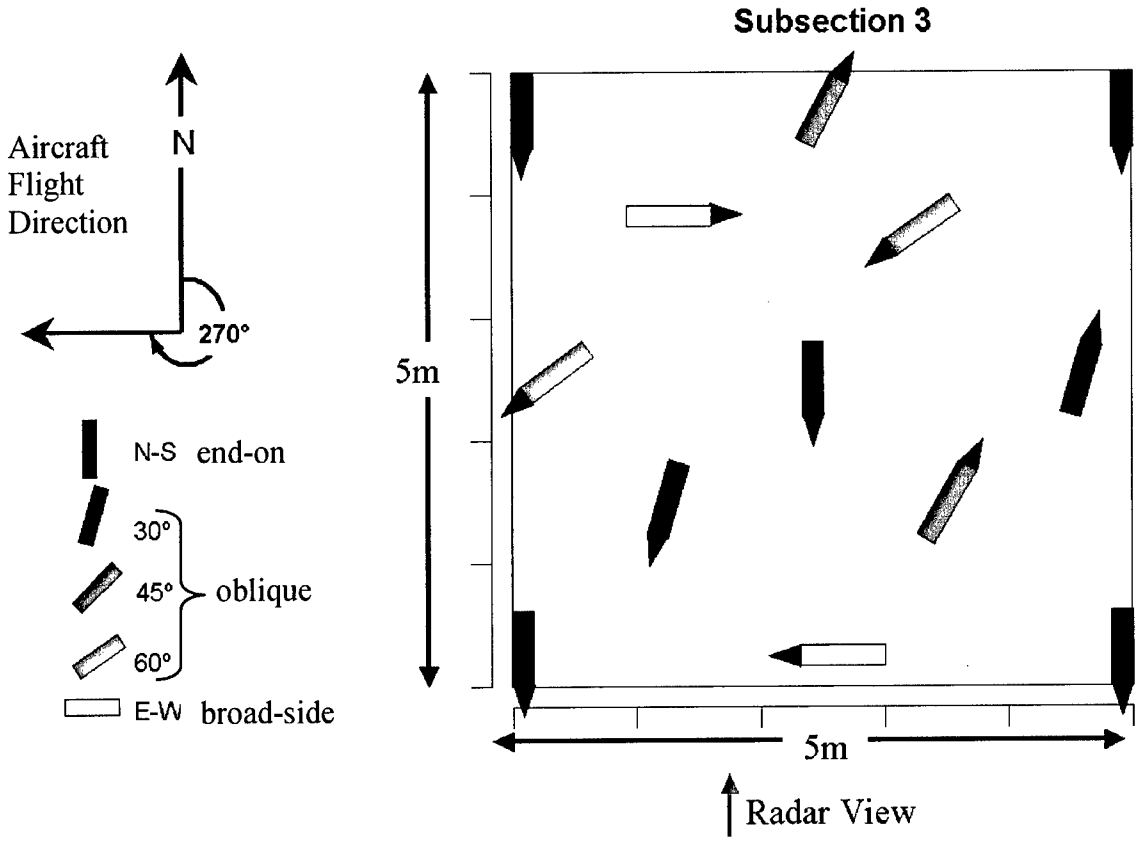

Figure 23. 155-mm projectile layout

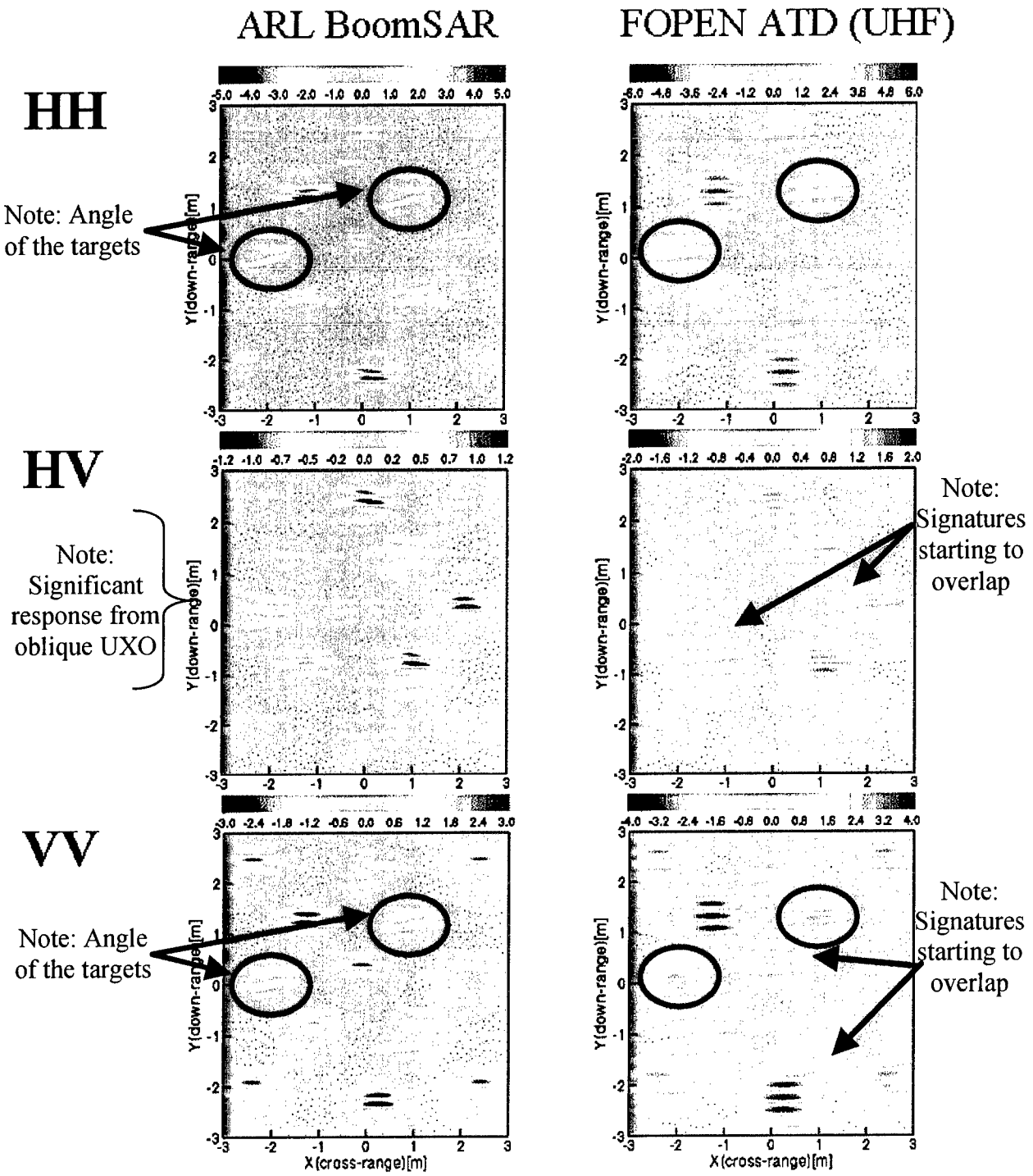

Figure 24. Simulated imagery for 155-mm projectiles, **Camp Navajo soil**

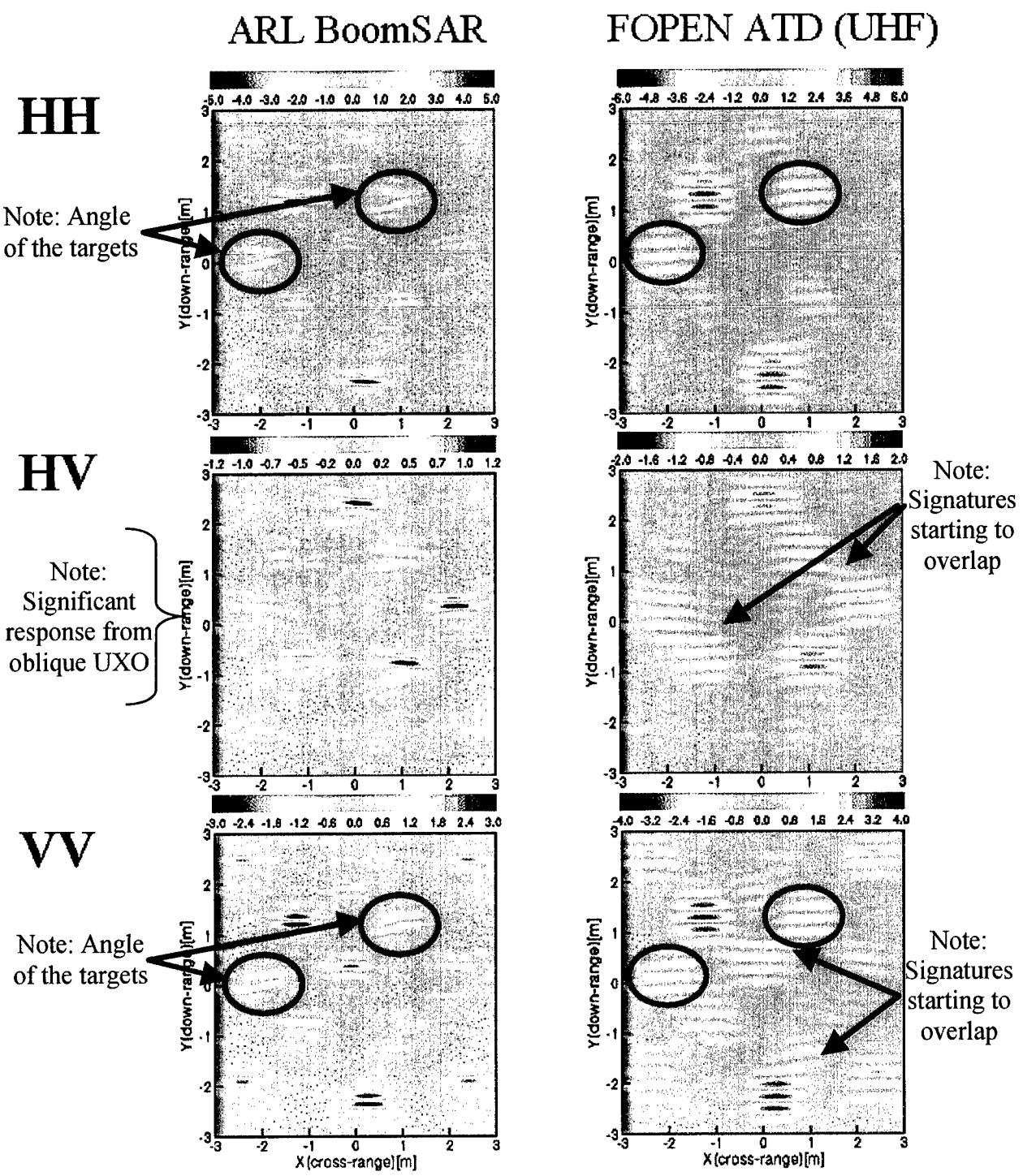

Figure 25. Simulated imagery for 155-mm projectiles, **Yuma soil**

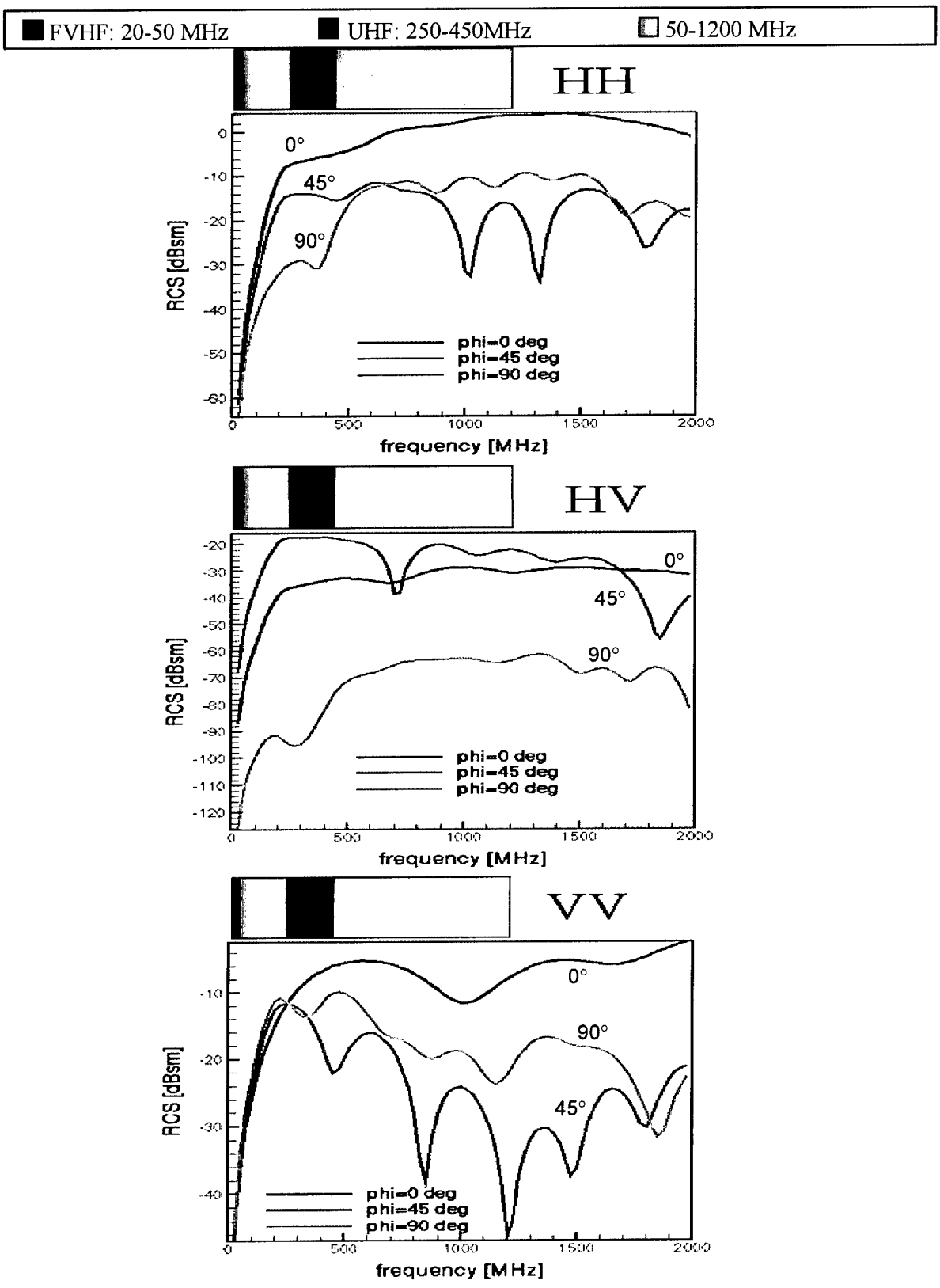

Figure 26. Frequency response of 155-mm projectile versus polarization and azimuth

Figures 24 and 25. This effect can also be seen in Figure 33 where the VHF signatures for the individual 2000-lb bombs are inseparable even when displayed on a 16-m × 16-m image area. Also, recall that the scales for the UHF and VHF plots in Figure 33 are different, and the VHF response is much lower. This becomes even worse when examining actual radar imagery as the FOPEN radar produces more power at UHF than it does at VHF. The loss of resolution means it will be extremely difficult to separate the returns from individual UXO in a collection of UXO, and difficult to separate UXO returns from those due to naturally occurring clutter (trees, large rocks, etc.).

5.1.4.3 Aspect Angle-Dependent Scattering. Figure 29 highlights the variability and uniqueness of angle-dependent scattering from UXO. The most obvious response is noted when the UXO is placed broadside to the radar viewing angle. This is encouraging not only because it is a large signature that may aid in cueing sensors to potentially contaminated areas, but it also may provide a unique signature that can distinguish it from other naturally occurring clutter. It has been reported that long, linear man-made objects exhibit a coherent phase structure across their complex image pixels, whereas naturally occurring clutter that may appear similar in the imagery does not exhibit this same phenomenon [10].

There is a significant response from the end-on targets as well. Also note that the position of these UXO may also produce a unique cross-polarized response (HV). The cross-polarized images in Figures 29 and 33 illustrate the 180-deg flip in the phase response as the radar passes through the axis of symmetry of the end-on targets. The image has alternating positive (red-yellow) and negative (blue) responses on one side of the target location, and the opposite pattern on the other side of the target, with a region of virtually no signal in the middle. The physical explanation for this pattern is that an end-on target is symmetric, and thus theoretically has zero cross-pol response. Most vertical cylinders exhibit this symmetry from all azimuth angles, and thus have no cross-pol response for any azimuth angle. However, once the radar aperture moves beyond perfect alignment with the longitudinal axis of the end-on target, it no longer appears symmetric, and target amplitude begins to increase (in addition to changing the sign of the electric field causing the phase change).

5.1.4.4 Polarization-Dependent Scattering. There are a number of interesting features visible in all of the images depending on the target orientation and the polarization. Typically, it is expected that simple targets such as these have the largest response in co-polarized (HH or VV) channels. Not surprisingly, the largest return in the HH image comes from the broadside target, and this can be seen even in the VHF imagery of the 2000-lb bomb (Figure 33). In the FOPEN UHF imagery shown in Figure 33 there is little response to the end-on targets in HH relative to the broadside targets. However, in VV, the end-on targets that are aligned with the incoming EM field are almost as bright as the broadside targets.

The cross-polarized response (HV) is always weaker than either of the co-polarized responses. However, if there is enough signal-to-noise available in the imagery, there are a number of common features noticeable here as well. Not surprisingly, the oblique targets are the brightest in the cross-pol images, because the cross-pol highlights the asymmetry of the targets (Figures 24, 25, 29, and 33).

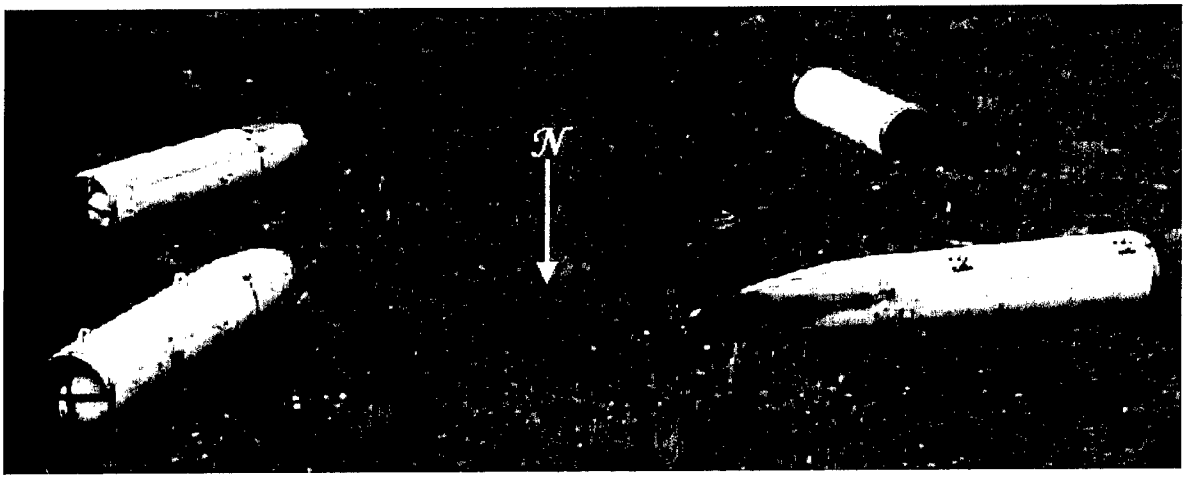

Figure 27. Photo of 500-lb bomb layout (note missing center bomb)

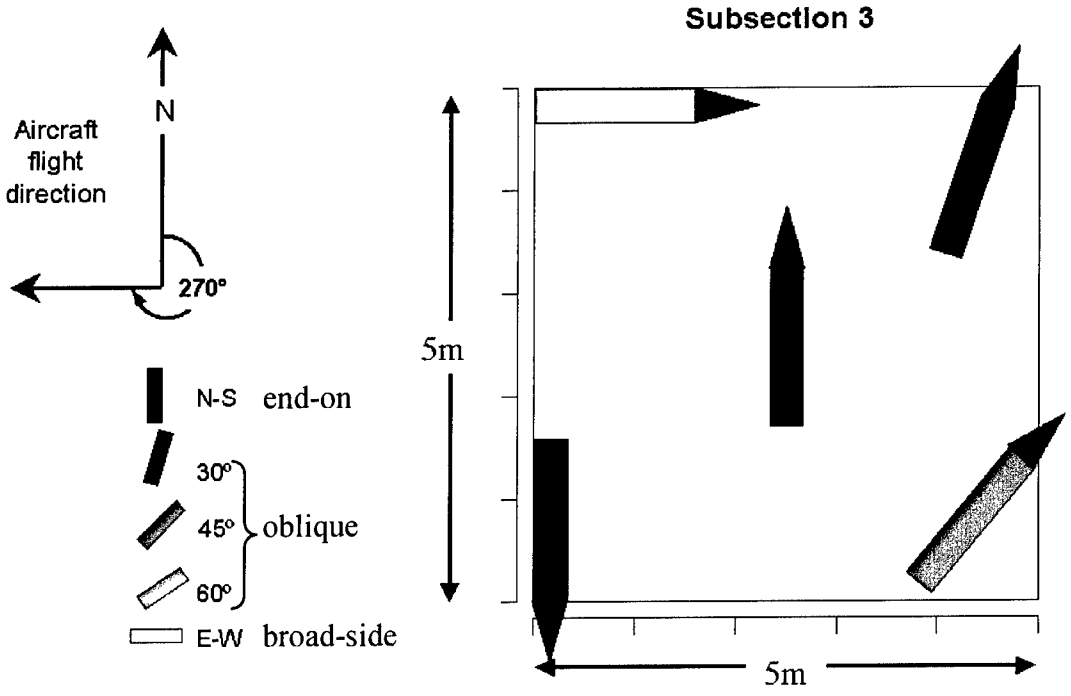

Figure 28. 500-lb bomb layout for EM model

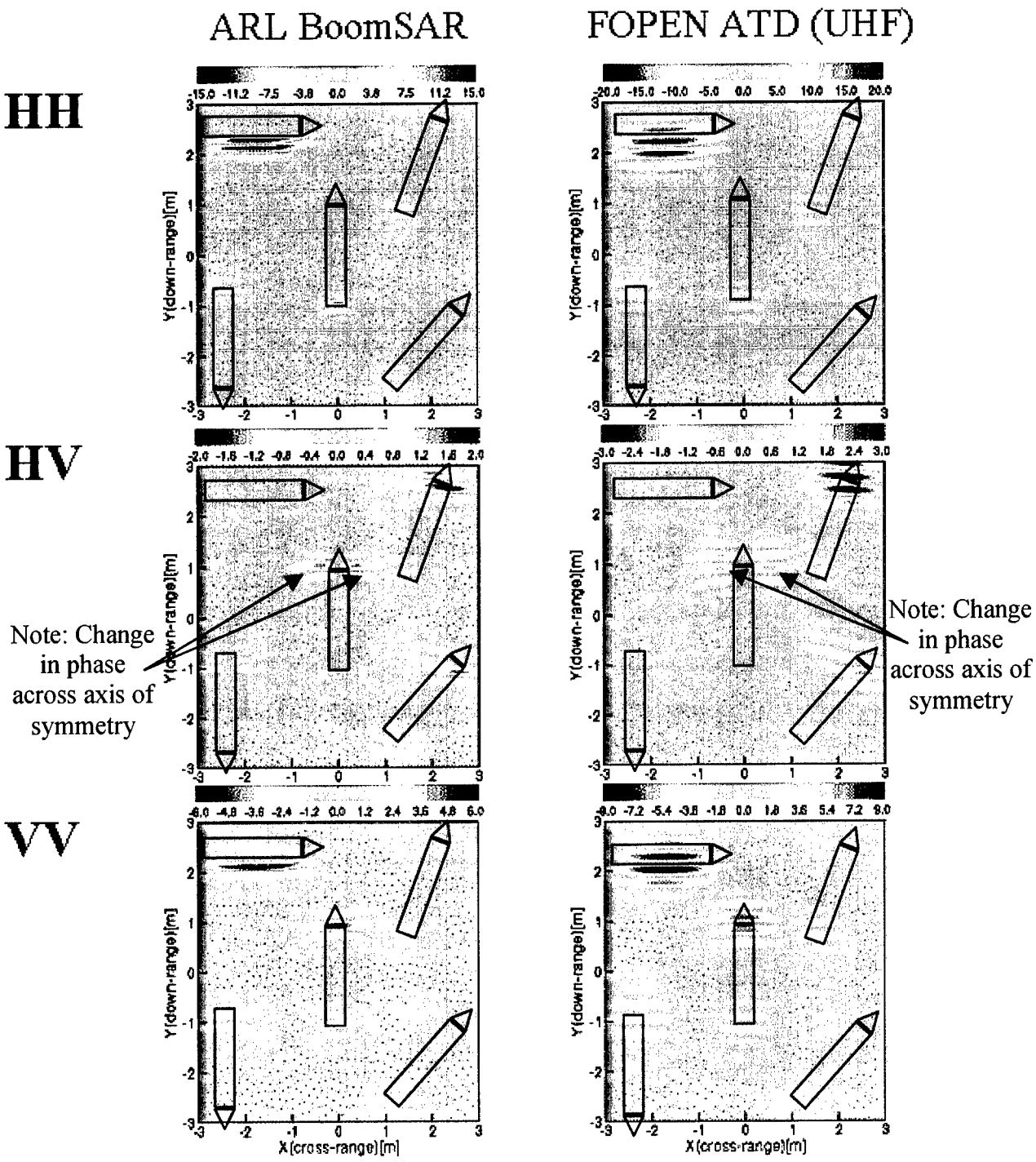

Figure 29. Simulated imagery for 500-lb bombs, Camp Navajo soil

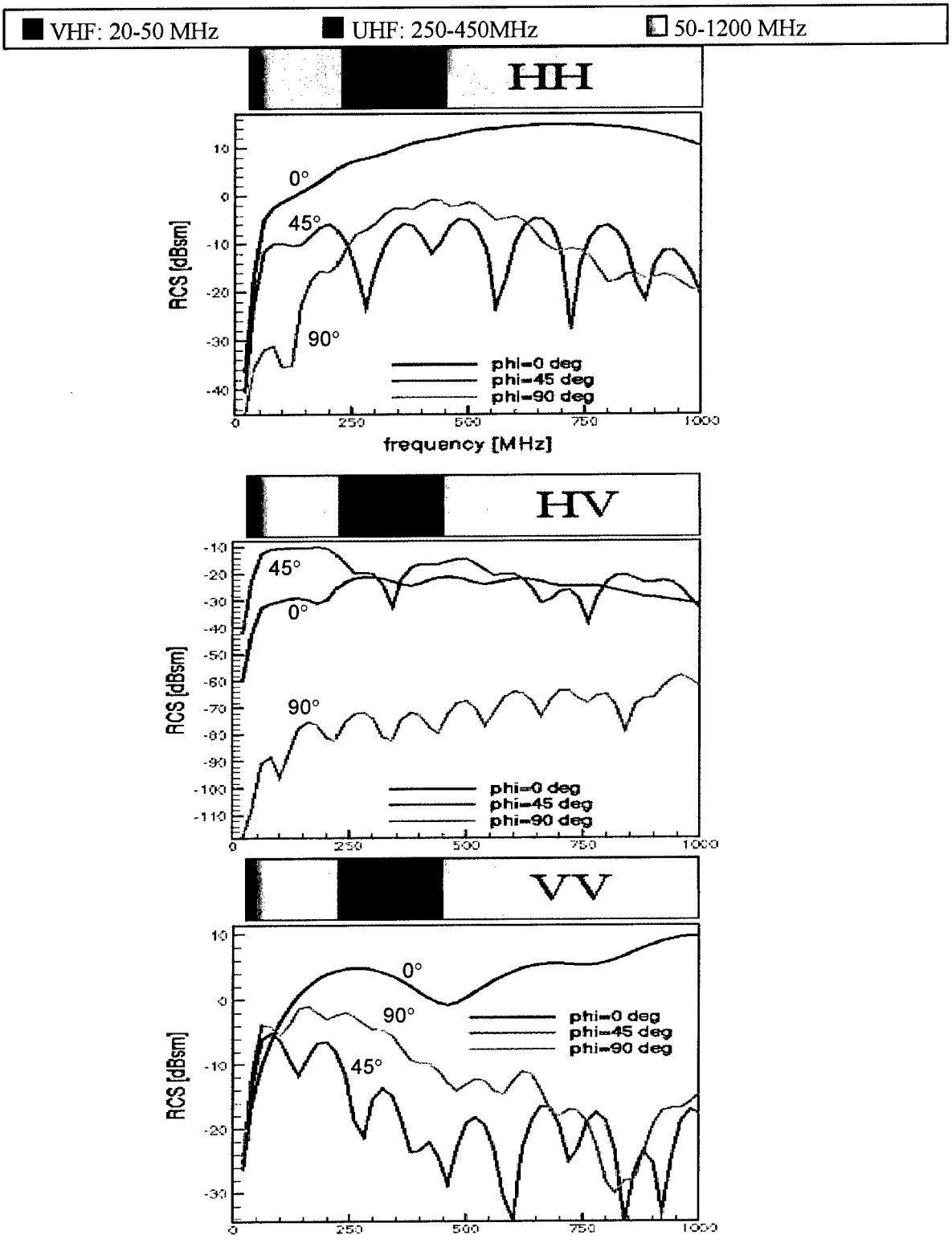

Figure 30. Frequency response of 500-lb bomb versus polarization and azimuth

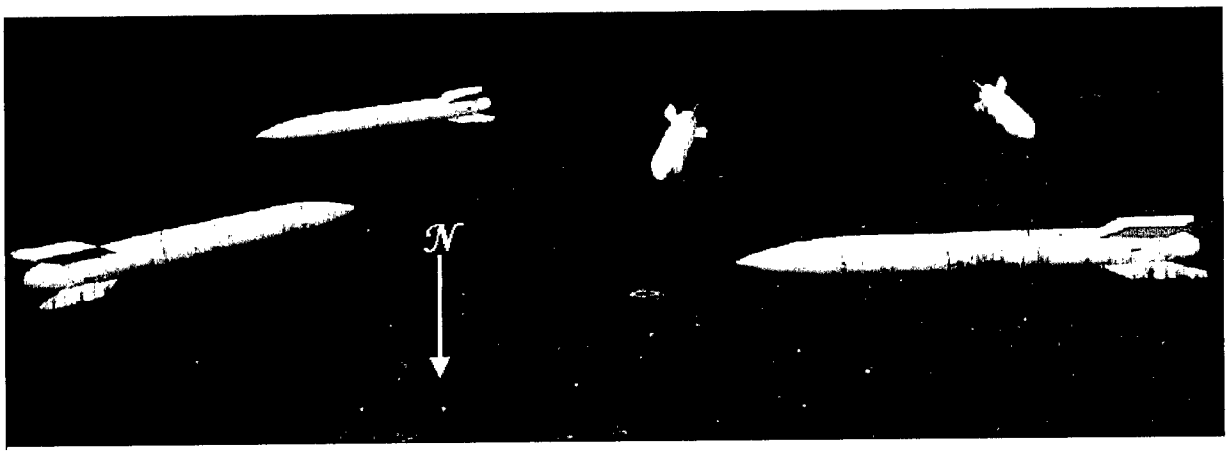

Figure 31. Photo of 2000-lb bomb layout at Camp Navajo

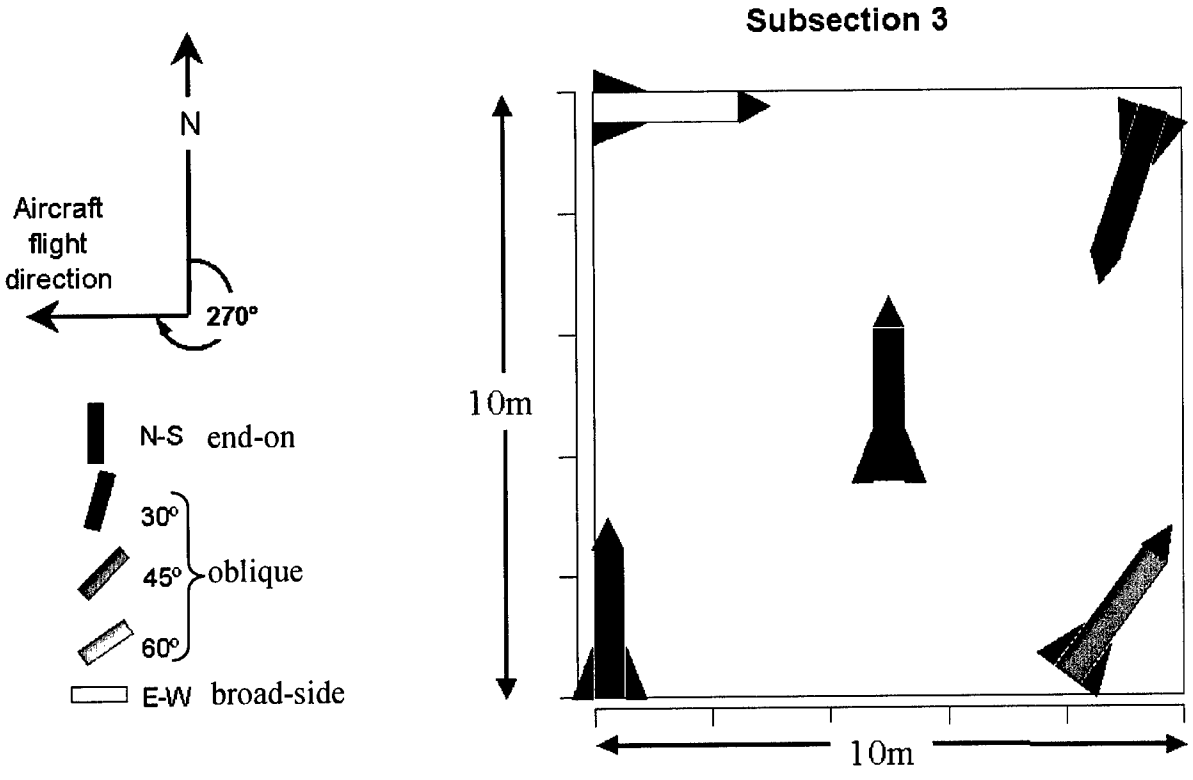

Figure 32. 2000-lb bomb layout

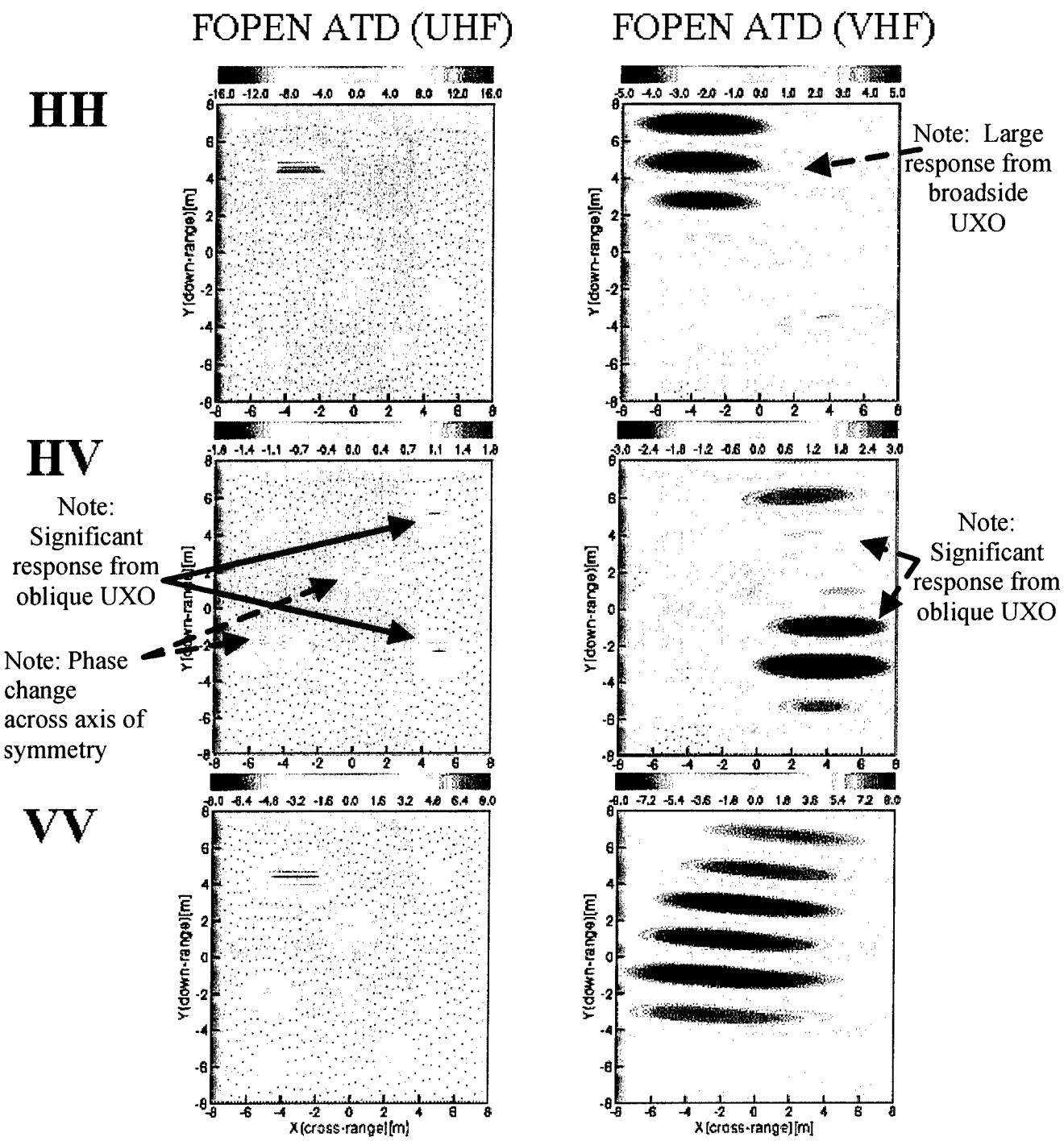

Figure 33. Simulated imagery for 2000-lb bombs, Camp Navajo soil

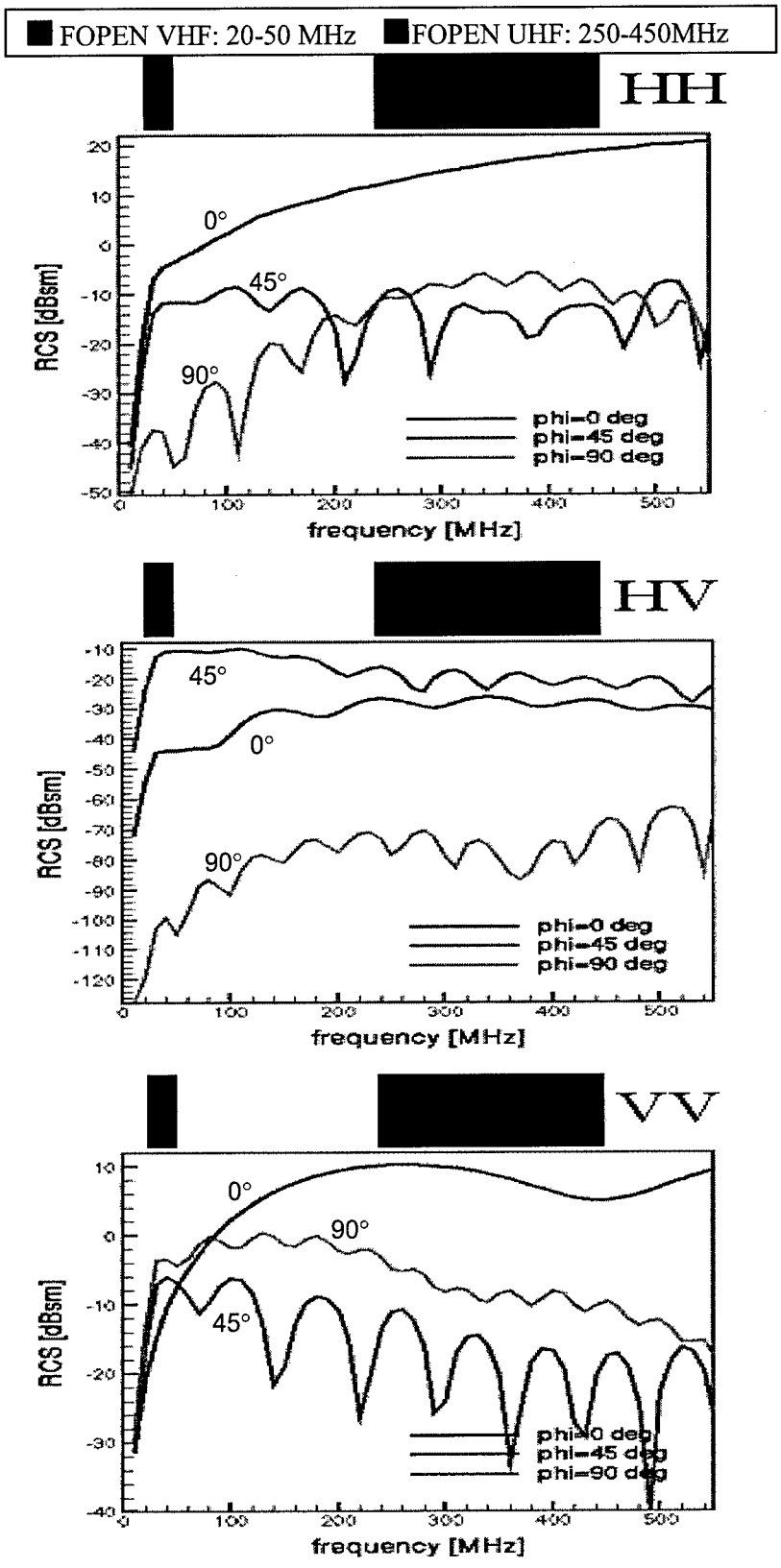

Figure 34. Frequency response of 2000-lb bomb versus polarization and azimuth

5.1.4.5 Frequency-Dependent Scattering The frequency plots in Figures 26, 30, and 34 were computed for three radar viewing angles (0-deg broadside, 45-deg oblique, 90-deg end-on). These figures quantitatively illustrate what was observed in the simulated SAR imagery. That is, the broadside UXO generates the largest response in the co-polarized channels (HH and VV) and the oblique UXO generates the largest response in the cross-polarized channels (HV). The structure of the response from the three UXO types appears to increase as the target gets larger. That is, there is more structure (peaks and valleys) for the 2000-lb bomb versus the 155-mm round. This direct relation between UXO size and frequency response could be used to discriminate one UXO type from another UXO type. It is also noted that the HV response of the end-on target is 50 dB smaller than the broadside and oblique targets.

5.2 Data Assessment

5.2.1 Imagery [1]. The initial results of the FOPEN ATD UHF imagery from the UXO *open* deployments are encouraging. Both the 2000- and 500-lb items are visible in the HH and VV polarization channels when the UXO orientation is parallel to the aircraft heading. Combining multiple look angles improves detection of the 2000- and 500-lb items. A T/C ratio greater than 20 dB in the dense deployments enabled detection of the UXO against the grass background. It may be possible to detect all targets with a lower T/C threshold, however other objects (trees, bushes, fences, etc.) would also be detected. It would be necessary to employ a discrimination stage (for example, a stage that looks for groups of detections with a certain minimum density that would signify a UXO impact area) to reduce detection of false alarms. Clusters of 155-mm projectiles are visible in the VV polarization data. The clutter background appears to have more influence on these smaller targets. *None of the targets,* even the larger 2000-lb bomb size, *were detectable under foliage.* For UXO proximal to trees, the T/C could drop 10 to 12dB, and if under trees, another 10-dB decrease is expected. The VHF data were found to be limited in UXO detection in this experiment because of insufficient resolution and the small RCS of the UXO targets at this frequency band. The FOPEN ATD UHF data were found to be limited by multiplicative noise as a result of spectral notching, which makes the detection of the dimmer UXO targets difficult.

5.2.2 Modeling. The modeling studies by ARL commenced prior to the completion of the image processing by MIT/LL. Because of this, ARL did not know which passes MIT/LL would eventually select for further processing. The images processed by MIT/LL span less than 40 deg in azimuth. Figure 35 shows plots of calculated RCS over a 40-deg range for the 2000-lb, 500-lb, and 155-mm target (Personal communication, 25 November 2002, Anders Sullivan, Electronics Engineer, Army Research Laboratory, Adelphi, MD). The 155-mm curve exhibits little to moderate variation whereas the 500-lb and 2000-lb curves vary significantly. The average RCS computed from each curve in Figure 35 (using the center frequency of the UHF portion of the FOPEN radar) is compared to the measured (MIT/LL) RCS in Table 8. Assuming the MIT/LL data are perfectly calibrated, uncertainties in the soil relative dielectric permittivity and target orientation relative to the flight path of the radar most likely account for the 4- to 5-dB discrepancy between the measured and modeled data. It is important to note that because the heading offset between the 0- and 30-deg flights and the integration angle (less than 40 deg) do

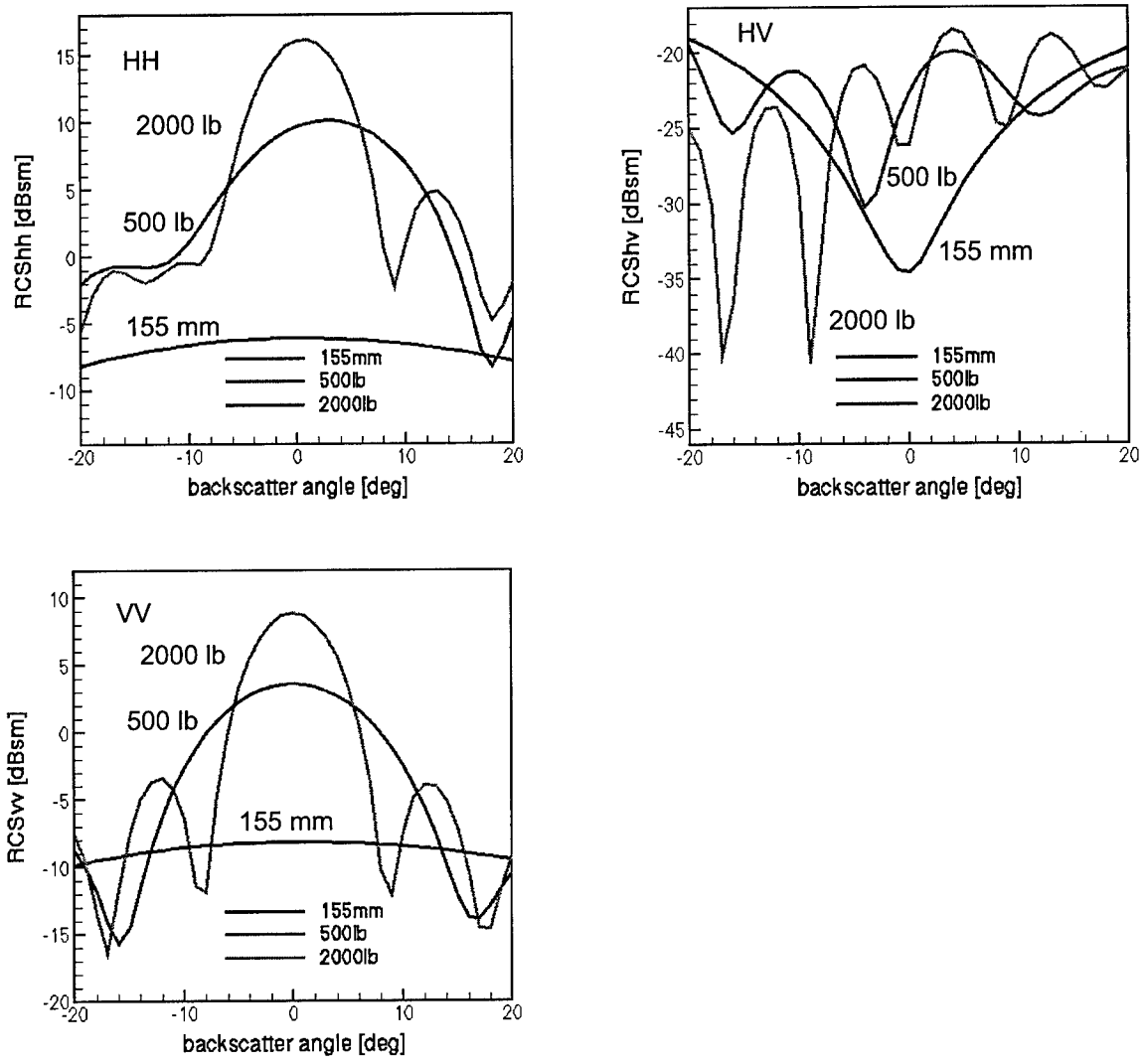

Figure 35. RCS of 155-mm shell, 500-lb bomb, and 2000-lb bomb as a function of azimuth angle

Table 8. Comparison of Measured and Modeled Average RCS over Notional 40-deg Azimuth Range

	155-mm Projectile		500-lb Bomb		2000-lb Bomb	
	Measured	**Model**	**Measured**	**Model**	**Measured**	**Model**
HH	-9.9	-6.7	0.4	5.9	5.7	9.4
HV	-19.4	-23.2	-18.0	-22.4	-11.5	-22.4
VV	-10.6	-8.6	-4.5	-0.7	-3.3	2.0

not sum to greater than 90 deg, it is not certain that the target was imaged broadside. To illustrate the importance of target orientation relative to the radar flight path, assume that there was a 20-deg heading offset so that the MIT/LL image was not formed evenly around the target broadside. This is illustrated in Figure 36. In this case, the RCS would be averaged over approximately –40 deg to 0 deg in azimuth. The average RCS values for this scenario are given in Table 9. The MIT/LL measurement values and the previous model averages are also given. The 20-deg heading offset is indicated by the "-40:0" label in the table, and the previous non-offset average is given by the "-20:20" label. As can be seen, the offset model results are closer to the MIT/LL measured data. This suggests that the image data are not purely broadside to the target and that the SAR models, given the uncertainties in the measurements, are representative of the radar system.

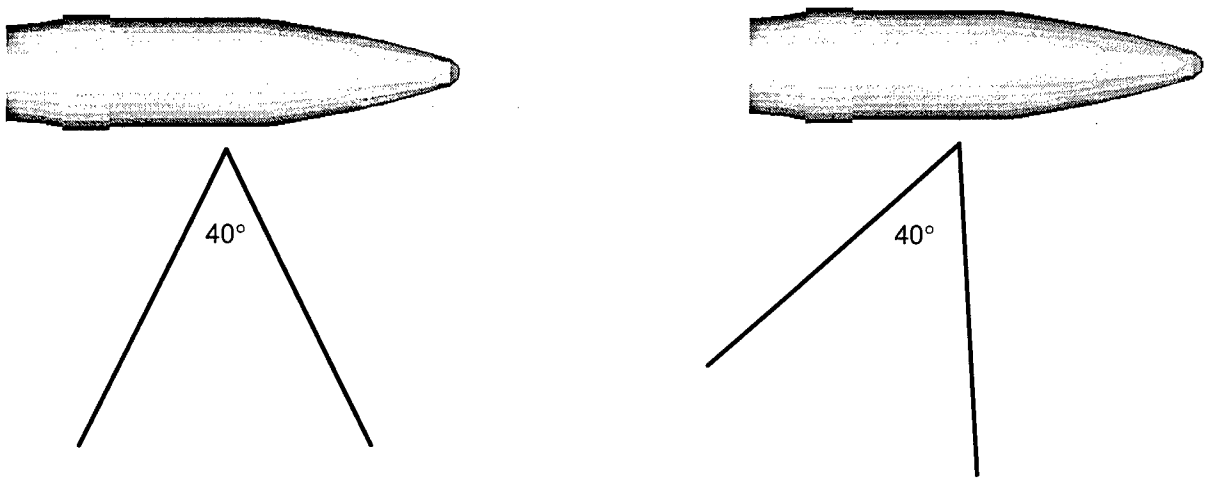

Figure 36. Target imaged around broadside (left) and with a 20-deg offset (right) for a notional 40-deg integration angle

Table 9. Comparison of Measured and Modeled Broadside and Offset Average RCS

	155-mm Projectile			500-lb Bomb			2000-lb Bomb		
	Measured	**-20:20**	**-40:0**	**Measured**	**-20:20**	**-40:0**	**Measured**	**-20:20**	**-40:0**
HH	-9.9	-6.7	-8.2	0.4	5.9	2.2	5.7	9.4	6.4
HV	-19.4	-23.2	-19.2	-18.0	-22.4	-20.0	-11.5	-22.4	-22.2
VV	-10.6	-8.6	-10.0	-4.5	-0.7	-2.9	-3.3	2.0	-0.3

5.3 Technology Comparison [3]

The mobile BoomSAR system (designed and constructed by ARL) allows data collection over a wide range of varying clutter and target-in-clutter scenarios to support phenomenology and target discrimination research. The BoomSAR emulates the collection geometries that can be achieved by a radar mounted on a helicopter or unmanned aerial vehicle (Figure 37). This radar covers 20 to 1100 MHz and the full polarization matrix to accomplish this task.

The radar is mounted atop a 150-ft (45.7-m) telescoping boom lift that can be driven forward while fully erect to permit the collection of synthetic aperture radar (SAR) data (Figure 38). This setup allows the system to emulate the imaging geometry of either an airborne or vehicle mounted radar. Further, it provides a high degree of control in the design and execution of test scenarios.

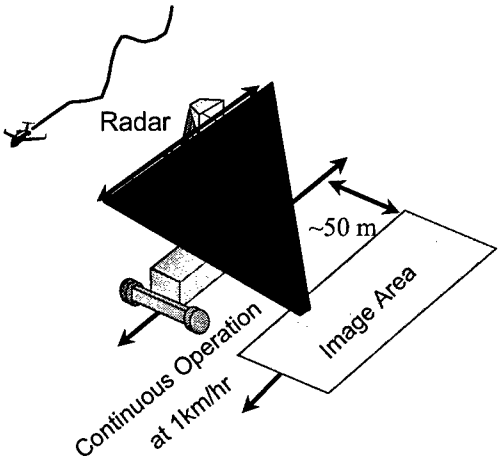

Figure 37. BoomSAR collection geometry

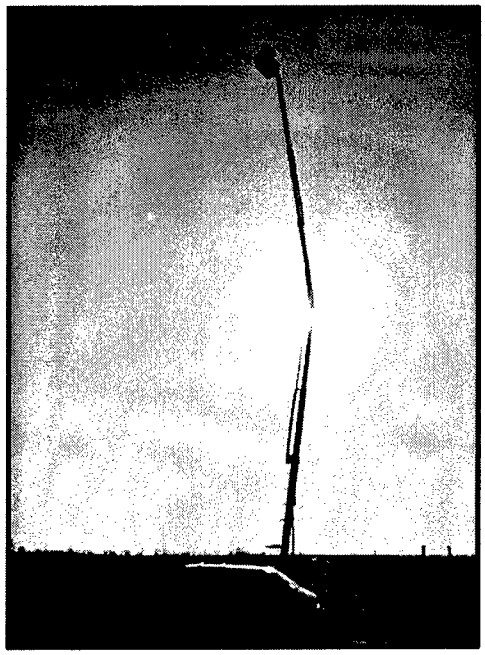

Figure 38. ARL BoomSAR system

The BoomSAR uses an impulse waveform with spectral response extending from 20 MHz to over 1 GHz. This 1-GHz bandwidth, which is directly digitized on receive, gives a measured 6-in. (15-cm) resolution in the range dimension. High resolution in the cross-range dimension is achieved with the use of SAR techniques to process those returns to achieve resolution as small as 11 in. (28 cm). The tabulation below highlights features of the BoomSar system.

Antenna	2 transmit, 2 receive
Frequency Coverage	20–1100+MHz
PRF	700 Hz
Polarization	HH,VV,HV,VH
Average Power	1 W
Waveform	Impulse
Receive Processing	Baseband Sampling; 8 Bit
Receiver AGC	Computer Control
Processed Range Gates	Scaleable: 4096 and up
Motion Compensation	Embedded in data stream
Platform Speed	1 km/hr

6. Cost Assessment

6.1 Cost Performance

Minimum cost for a single flight of the FOPEN SAR system is approximately $150k. That cost includes: (a) estimated flight cost of $10k per flight, with a flight consisting of five passes, which includes processed imagery of each pass; (b) ground truth costs estimated at $40k; (c) additional image processing performed by MIT/LL at approximately $20k per pass. Recent improvements in image processing have likely eliminated the need for the additional processing by MIT/LL, making the flight cost $100k or less.

6.2 Cost Comparisons to Conventional and Other Technologies

Conventional ground-based radar systems are not feasible for exploration purposes involving multiple hectares.

7. Regulatory Issues

7.1 Approach to Regulatory Compliance and Acceptance

This project had no direct involvement with regulators or the public.

8. Technology Implementation

8.1 DoD Need

The Army has identified UXO cleanup as its highest priority Environmental Restoration problem. As much as 15 million acres (6 hectares) in the United States may be contaminated with UXO [11]. UXO vary in size from 20-mm to 2000-lb bombs and may be found buried to a depth of 10-m. Currently the DoD spends millions of dollars annually on the remediation of UXO contaminated sites.

8.2 Transition

Further testing is required to determine if the FOPEN SAR system is capable of imaging buried UXO and its limitation of detecting UXO in a variety of foliage types (short grasses, long grasses, small brush, sparsely planted forest, etc.). Flights over established UXO and mine test sites would provide a valuable data set for image processing and modeling studies. Some established test sites are located at: (a) UXO: Aberdeen Proving Ground, Yuma Proving Ground; (b) Mine: Yuma Proving Ground, Fort A.P. Hill.

The data from Camp Navajo are available to begin studies on advanced processing techniques (i.e., polarimetric, multilook, and superresolution) and system trade-offs. A study is recommended to define a better impact area detection system. Factors to optimize are resolution, frequency band, and system sensitivity.

Now that the high-fidelity EM models exist, more work is necessary to define robust unique signatures of UXO. Once a unique signature is identified, the models can incorporate the noise, interference, and inaccuracies present in real airborne data collections to determine the level of imperfection in radar performance that can be tolerated in order to still acquire the unique UXO feature.

9. Lessons Learned

Large targets (bomb-size) and dense collections of smaller (155-mm) targets can be detected by the UHF FOPEN SAR when located on the ground surface within sparsely vegetated areas. Multiple aircraft headings will likely increase the chance of imaging UXO. Trees proximal to targets degraded the target resolution and no targets under foliage were able to be resolved. An airborne SAR system with greater resolution is desirable. There is a trade-off between optimizing a system for foliage penetration and one that is optimized for the detection of UXO-size targets. A combination of frequency, polarization, and angle-dependent scattering features may allow separation of UXO from clutter when the UXO has a reasonable length-to-diameter ratio and is still basically intact. To determine the usefulness of these features, more work is needed to determine how to exploit effective combinations of them in automatic detection algorithms. With the modeling software and image processing techniques now available, studies

should be conducted to determine a set of SAR system parameters that would be applicable for detecting UXO in various terrain conditions.

10. References

1. L.A. Bessette. 2002. *FOPEN ATD Camp Navajo UXO Data Collection Summary.* Massachusetts Institute of Technology Lincoln Laboratory, Project Report FPR-22, 4 June 2002.

2. L. Carin. 2002. *Duke Final Report on ESTCP SAR Project.* Department of Electrical and Computer Engineering, Duke University, 2002.

3. A. Sullivan, K. Kappra, and M. Ressler. 2002. *Electromagnetic Model Predictions of the Unique Frequency, Angle, and Polarization Dependent Signatures of Unexploded Ordnance.* Army Research Laboratory, 2002.
4. U.S. Army Environmental Center. 2002. *FY02 Army Environmental Requirements and Technology Assessments (AERTA).* SFIM-AEC-PC-CR-2002040, Final Report October 2002.

5. J.E. Simms. 2001. *ESTCP Flight Test Plan, Camp Navajo, AZ.* U.S. Army Engineer Research and Development Center, Vicksburg, MS 39180-6119.

6. R. Goodman, S. Tummala, and W. Carrara. 1995. *Issues in Ultra-Wideband, Widebeam SAR Image Formation.* Proc. IEEE 1995 Int. Radar Conf., 479485, 8-11 May 1995, Alexandria, Va.

7. L.A. Bessette, M.F. Toups, and B.T. Binder. 1996. *Documentation of the Lincoln Laboratory Processing for P-3 UWB SAR Imagery.* MIT Lincoln Laboratory Project Memorandum 47PM-STD-0010, 21 August 1996.

8. A.F. Yegulalp. 1999. *Fast Backprojection Algorithm for Synthetic Aperture Radar.* Proc. 1999 IEEE Int. Radar Conf., 60–65, 20–22 April 1999, Waltham, Mass.

9. L.M. Novak and M.C. Burl. 1990. *Optimal Speckle Reduction in Polarimetric SAR Imagery.* IEEE Trans. Aerosp. Elec. Sys., March 1990.

10. Jen King Jao, Serpil Ayasli. 1995. *SAR Detection of Wires Using Image Phase Signatures.* Record of the IEEE International Radar Conference, pp. 362-368, May 1995.

11. Defense Science Board. 1998. *Task Force Report on Unexploded Ordnance (UXO) Clearance, Active Range UXO Clearance, and Explosive Ordnance Disposal (EOD) Programs.* Task Force Report to the Office of the under Secretary of Defense (Acquisition and Technology), April 1998.

Appendix A
Points of Contact

Project Manager: Janet Simms, U.S. Army Engineer Research and Development Center, 3909 Halls Ferry Road, Vicksburg, MS 39180-6199; (601)634-3493; (601)634-3453 fax; Janet.E.Simms@erdc.usace.army.mil

Participating Organizations

Army Research Laboratory, ATTN AMSRL SE RU, 2800 Powder Mill Road, Adelphi, MD 20783; Karl A. Kappra, (301)394-0848; (301)394-4690 fax; kkappra@arl.army.mil
Computer modeling

DARPA IXO, 3701 N. Fairfax Drive, Arlington, VA 22203-1714; Lee Moyer; (703)696-2247; (703)741-1390 fax; lmoyer@darpa.mil
FOPEN SAR Program Manager

Duke University, Department of Electrical and Computer Engineering, Box 90291, Durham, NC 27708-0291; Dr. Lawrence Carin; (919)660-5270; (191)660-5293 fax; lcarin@ee.duke.edu
Software development

Lincoln Laboratory Massachusetts Institute of Technology, 244 Wood Street, Lexington, MA 02420-9108; Dr. Serpil Ayasli; (781)981-7440; (781)981-0300 fax; serpil@ll.mit.edu
Image processing

Appendix B
Data Archiving and Demonstration Plan

The radar data and auxiliary data from the FOPEN SAR UXO flight at Camp Navajo, Arizona, is being archived at both the Sensor Data Management System (SDMS) at the Air Force Research Laboratory (AFRL) and at Solers, Inc, in Arlington, VA. In addition, Lockheed Martin also maintains a master copy of all the FOPEN SAR data collected. SDMS is currently funded to distribute complex imagery and raw data from the FOPEN SAR, including the UXO flight data from Camp Navajo (upon permission from the ESTCP office).

The information archived at SDMS and Solers includes the (a) raw VHF and UHF data collected by the FOPEN SAR, along with the data from the onboard integrated GPS/Inertial Navigation System (INS) motion measurement subsystem, and the differential GPS solution generated post-flight; (b) complex calibrated UHF and VHF imagery generated by Lockheed Martin; (c) set of documents describing the sensor parameters used during the data collection and the ground truth information; and (d) documentation package describing the format of the auxiliary data and raw data files and providing example software (matlab files) for opening/reading the raw and auxiliary data files and doing the range-compression component of the image formation processing.

The demonstration plan can be obtained from the Program Manager point of contact listed in Appendix A.

Appendix C
Description of Select Image Processing Technical Terms

Average clutter backscatter coefficient (dB): calculated by averaging log-scaled σ_o values.

Average tree backscatter coefficient (dB): clutter backscatter coefficient calculated from homogeneous tree region of image; used for checking calibration accuracy and measuring CNR (clutter-to-noise ratio).

Clutter backscatter coefficient σ_0 (dB): calculated by dividing the measured RCS of each resolution cell by the ground-plane resolution cell area. Computed for areas of homogeneous clutter (trees or grass).

Clutter mean (dBsm): mean computed from the log-scaled RCS values of a clutter region.

Clutter standard deviation σ_c (dB): computed from the log-scaled RCS values of a clutter region; used in determining detection levels.

CNR (dB): clutter-to-noise-ratio; average tree backscatter coefficient-to-noise ratio; removes pass-to-pass calibration variation; indicates image noise levels.

Noise equivalent σ_0 (dB): average noise level in image; measured from low return area in image (a region of calm water is preferred). In the FOPEN ATD data, the returns from grass areas indicate the image noise equivalent σ_o. Image noise may be due to a combination of factors such as system noise, residual radio frequency interference (RFI) that was not removed during processing, multiplicative noise contamination due to spectral notching, or backlobe contamination.

T/C (dB): peak target to mean clutter ratio; log (RCS target peak) minus clutter mean; removes any pass-to-pass calibration variation; used in determining detection levels.

REPORT DOCUMENTATION PAGE

Form Approved
OMB No. 0704-0188

1. REPORT DATE *(DD-MM-YYYY)*	2. REPORT TYPE	3. DATES COVERED *(From - To)*
August 2003	Final report	

4. TITLE AND SUBTITLE

Applications of Synthetic Aperture Radar (SAR) to Unexploded Ordnance (UXO) Delineation

5a. CONTRACT NUMBER

5b. GRANT NUMBER

5c. PROGRAM ELEMENT NUMBER

6. AUTHOR(S)

Janet E. Simms

5d. PROJECT NUMBER

5e. TASK NUMBER

5f. WORK UNIT NUMBER

7. PERFORMING ORGANIZATION NAME(S) AND ADDRESS(ES)

U.S. Army Engineer Research and Development Center
Geotechnical and Structures Laboratory
3909 Halls Ferry Road
Vicksburg, MS 39180-6199

8. PERFORMING ORGANIZATION REPORT NUMBER

ERDC/GSL TR-03-15

9. SPONSORING / MONITORING AGENCY NAME(S) AND ADDRESS(ES)

U.S. Army Corps of Engineers
Washington, DC 20314-1000;
Environmental Security Technology Certification Program
901 North Stuart Street, Suite 303
Arlington, VA 22203

10. SPONSOR/MONITOR'S ACRONYM(S)

11. SPONSOR/MONITOR'S REPORT NUMBER(S)

ESTCP #200126

12. DISTRIBUTION / AVAILABILITY STATEMENT

Approved for public release; distribution is unlimited

13. SUPPLEMENTARY NOTES

14. ABSTRACT

The Environmental Security Technology Certification Program (ESTCP) provided funding to determine the feasibility of using a foliage penetration (FOPEN) synthetic aperture radar (SAR) system to delineate unexploded ordnance (UXO) contaminated areas. The FOPEN SAR system was developed under a program funded by the Defense Advanced Research Projects Agency(DARPA), Army, and Air Force. The U.S. Army Engineer Research and Development Center coordinated the project efforts, which included participation of the Massachusetts Institute of Technology Lincoln Laboratory, Duke University, and the U.S. Army Research Laboratory. The objective was to measure UXO target signatures in varying target placement conditions, including target orientation, proximity to other targets, and foliage coverage. Three target sizes were imaged; 155-mm projectiles and simulants representing a 2000-lb bomb and 500-lb bomb. Large targets (bomb-size) and dense collections of smaller (155-mm) targets can be detected by the UHF FOPEN SAR when located on the ground surface within sparsely vegetated areas. Multiple aircraft headings will likely increase the chance of imaging UXO. Trees proximal to targets degraded the target resolution and no targets under foliage were able to be resolved. Environmental restrictions at the test site (Camp Navajo, Arizona) prohibited the burying of targets so no statements regarding the FOPEN SAR imaging capabilities of buried UXO can be made. The FOPEN SAR is not optimized for UXO detection. Optimizing the frequency range of a SAR system and exploiting polarization and angle-dependent scattering features may allow separation of UXO from clutter.

15. SUBJECT TERMS

Foliage penetration
Geophysics
SAR
Synthetic aperture radar
Unexploded ordnance
UXO

16. SECURITY CLASSIFICATION OF:			17. LIMITATION OF ABSTRACT	18. NUMBER OF PAGES	19a. NAME OF RESPONSIBLE PERSON
a. REPORT	b. ABSTRACT	c. THIS PAGE			19b. TELEPHONE NUMBER *(include area code)*
UNCLASSIFIED	UNCLASSIFIED	UNCLASSIFIED		67	